

# Outage Constrained Robust Transmission Design for IRS-aided Secure Communications with Direct Communication Links

Sheng Hong, Cunhua Pan, Gui Zhou, Hong Ren, and Kezhi Wang

## Abstract

In this paper, we investigate the robust outage constrained transmission design for an intelligent reflecting surface (IRS) aided secure communication system. We assume that a single-antenna legitimate receiver (Bob) served by a multi-antenna base station (BS) is overheard by multiple single-antenna eavesdroppers (Eves), and the artificial noise (AN) is incorporated to confuse the Eves. In particular, we aim to jointly optimize the transmit beamforming, the AN spatial distribution at the BS, and the passive beamforming at the IRS, where the Eve-related channels are assumed to be imperfect due to the channel estimation errors and their concealment. Two scenarios with partial channel state information (CSI) error of only cascaded BS-IRS-Eve channel and full CSI errors of both cascaded BS-IRS-Eve channel and direct BS-Eve channel are investigated under the statistical CSI error model. An outage-constrained power minimization problem is formulated by limiting the maximum allowable data rate of Eves and ensuring the minimum data rate requirement of Bob. To solve it, the Bernstein-type inequality and alternating optimization strategy are exploited, and artful mathematical manipulations are performed to facilitate the optimization on the phase shifts of the IRS. Simulation results confirm the performance advantages of the proposed algorithm.

## Index Terms

Intelligent Reflecting Surface (IRS), Reconfigurable Intelligent Surface (RIS), Robust design, Imperfect CSI, Physical Layer Security, Secure Communications.

S. Hong is with Information Engineering School of Nanchang University, Nanchang 330031, China. (email: shenghong@ncu.edu.cn). C. Pan and G. Zhou are with the School of Electronic Engineering and Computer Science at Queen Mary University of London, London E1 4NS, U.K. (e-mail: {c.pan, g.zhou}@qmul.ac.uk). H. Ren is with the National Mobile Communications Research Laboratory, Southeast University, Nanjing 210096, China. (hren@seu.edu.cn). K. Wang is with Department of Computer and Information Sciences, Northumbria University, UK. (email: kezhi.wang@northumbria.ac.uk). (Corresponding author: Cunhua Pan)

## I. INTRODUCTION

The intelligent reflecting surface (IRS), also known as reconfigurable intelligent surface (RIS), is a promising technique in future six generation (6G) communication networks [1], [2]. The IRS consists of a large number of reflecting elements, each of which can reflect the incident signal with a reflecting coefficient [3]. By properly controlling the reflecting coefficients, the reflected signals can be added constructively at the desired receiver for enhancing the received signal power, or destructively at the non-intended receivers for suppressing interference [1]. There are appealing advantages of the IRS technique. Firstly, an IRS can intelligently configure the wireless environment to help the transmissions between the sender and the receiver, especially when direct communication links are in poor quality. The reflecting element of the IRS operates in a passive mode without any radio frequency (RF) chain, thus deploying an IRS costs much less than deploying a relay [4]. Since the IRS only reflects incident signals, it can significantly improve the spectral and energy efficiency of the wireless networks. The IRS normally has light weight and compact size, thus it can be readily installed on building facades, interior walls, room ceilings, lamp posts and road signs with low cost. Meanwhile, it can be easily integrated into traditional communication systems with only minor modifications. Therefore, the IRS-aided wireless communications have received extensive research attention, e.g. multicell networks [5], wireless power transfer design [6], mobile edge computing [7], multigroup multicast communication [8], and cognitive radio system [9].

Recently, the IRS has been proposed to deploy in conventional wireless networks to enhance the physical layer security performance. By jointly optimizing the beamforming vector at the transmitter and phase shifts at the IRS, the physical layer security can be significantly improved [10]–[12]. In [13], an IRS was applied to tackle the challenging scenarios where the channel of the legitimate communication link and that of the eavesdropping link are highly correlated. The authors in [14] showed that the advantages of joint use of an IRS and artificial noise (AN) are obvious when the number of eavesdroppers is large. A special scenario where the Eves are closer to the base station (BS) than the desired users was investigated by employing an IRS in [15], [16]. The work in [17] verified the performance enhancement by using an IRS in a challenging scenario where the direct links from the BS to the users and the Eves are blocked.

However, all the above-mentioned papers were based on the assumption that the channel state information (CSI) associated with all involved channels is perfectly known at the BS, which is too idealistic. In practice, it is challenging to obtain the perfect CSI in IRS-aided communications,

since the IRS is passive that does not employ any RF chains [1], [2]. The current contributions on the channel estimation (CE) for the IRS-related channels can be divided into two methods. The first method is to estimate BS-IRS channel and IRS-user channel separately [18]. The main idea of this method is to install some active channel estimators at the IRS, and then estimate the BS-IRS channel and IRS-user channel individually, and finally send the estimated channels to the BS. The second method is to estimate the cascaded channels directly [19]–[22]. The cascaded BS-IRS-user channel is the product of the BS-IRS channel and IRS-user channels, which is sufficient for the joint optimization of active and passive beamforming [8], [23]. The second estimation method is more attractive than the first method, because no additional active hardware is required, and no additional power is consumed. Moreover, the channel training and feedback overhead is reduced in the second method.

However, the channel estimation error is unavoidable. The system will suffer performance degradation if naively treating the estimated channels as perfect ones. Thus it is imperative to take the CSI error into consideration, and design the robust transmission strategy in IRS-aided communications. To the best of our knowledge, there are only a paucity of contributions devoted to this area. In [24], a worst-case robust design algorithm was proposed by considering the imperfect IRS-user channels in a multiuser MISO communication system. In [25], a worst-case robust design in IRS-assisted secure communications was firstly investigated, where the IRS-Eve channels were assumed to be imperfect and the direct links from BS to users were blocked. The robust transmission design in these two contributions rely on the first CE method, which may not be an appealing CE method. The robust transmission design based on the second CE method was firstly proposed in [26], where the cascaded BS-IRS-user channels at the transmitter were imperfect, and both the bounded CSI error and the statistical CSI error were investigated. Based on the second CE method, a worst-case robust transmit power minimization problem was investigated for the IRS-aided green MISO communications with both direct links and reflecting links [27], and a robust probabilistic-constrained transmit power minimization problem was investigated for IRS-aided MISO communications without direct links [28]. The authors in [29] considered the robust beamforming design in IRS-aided cognitive radio systems for imperfect cascaded CSI on primary user(PU)-related channels. In [30], we investigated the robust transmission design in IRS-assisted secure communications by assuming that the cascaded BS-IRS-Eve channels were imperfect, and the statistic CSI error model was adopted. However, the direct communication links in [30] were

assumed to be blocked, which is only applicable for some special scenarios.

Against the above background, this paper studies the outage constrained robust (OCR) transmission design by assuming that the cascaded BS-IRS-Eve channels are imperfect, and that there exist the direct links from the BS to users. An outage-constrained power minimization (OC-PM) problem is formulated to optimize the beamforming vector, the AN covariance matrix, and the phase shifts matrix of the IRS subject to the outage constraint of maximum information leakage to the eavesdroppers. The contributions of this work are summarized as follows:

- 1) To the best of our knowledge, this is the first work to study the outage constrained robust secure transmission for IRS-aided wireless communications by considering the direct communication links. In contrast to [25] and [30] that the direct BS-users links are assumed to be blocked, we are the first to investigate the robust transmission design in a more general and practical scenario with both direct links and IRS reflecting links.
- 2) We consider two kinds of scenarios where only the CSI errors exist for cascaded channels (i.e. partial CSI errors) as well as for both the cascaded channels and direct channels (i.e. full CSI errors).
- 3) Then, the Bernstein-type inequality (BTI) [31] is exploited, and the AO strategy is utilized to transform the original problems into two subproblems, where the solution to beamformer and the AN covariance matrix at the BS are obtained by using semidefinite relaxation (SDR) methods. For the nonconvex unit modulus constraints of IRS phase shifts, a penalty convex-concave procedure (CCP) [26] is explored.
- 4) The formulated problem is difficult to solve, since all the constraints become nonconvex with respect to (w.r.t.) the phase shifts of the IRS. To overcome this difficulty, complicated and artful mathematical manipulations are used to transform these constraints into convex ones.
- 5) Simulation results demonstrate that under both the partial CSI errors and full CSI errors, the proposed OCR transmission design algorithm can significantly reduce the transmit power while guaranteeing the secrecy rate constraints. Moreover, the proposed algorithm outperforms the benchmark schemes.

*Notations:* In this paper, vectors, matrices, and scalars are denoted by boldface lower case, boldface upper case and regular letters, respectively.  $(\cdot)^T$ ,  $(\cdot)^H$  and  $(\cdot)^*$  denote the transpose, Hermitian and conjugate operators, respectively.  $\text{Tr}(\mathbf{X})$  and  $|\mathbf{X}|$  denote the trace and determinant of  $\mathbf{X}$ , respectively.  $\mathbb{C}^{M \times N}$  represents the space of  $M \times N$  complex matrices.  $\text{Re}\{\cdot\}$  extracts the real part

of a complex value, and  $\text{diag}(\cdot)$  constructs a diagonal matrix.  $\mathcal{CN}(\boldsymbol{\mu}, \mathbf{Z})$  represents a circularly symmetric complex gaussian (CSCG) random vector with mean  $\boldsymbol{\mu}$  and covariance matrix  $\mathbf{Z}$ .

## II. SYSTEM MODEL

### A. Signal transmission model

As shown in Fig. 1, a multi-antenna transmitter, called Alice, intends to send confidential information to a single-antenna legitimate receiver, called Bob, in the presence of  $K$  single-antenna eavesdroppers, called Eves. Alice is equipped with  $N_t$  antennas, and the IRS is equipped with  $M$  programmable phase shifters to enhance the system security performance. By denoting the set of Eves as  $\mathcal{K} = \{1, 2, \dots, K\}$ , the received signals at Bob and Eves can be respectively modeled as

$$y_b = \hat{\mathbf{h}}_b^H \mathbf{x} + n_b = (\mathbf{h}_{ab}^H + \mathbf{h}_{rb}^H \boldsymbol{\Phi} \mathbf{G}_{ar}) \mathbf{x} + n_b, \quad (1a)$$

$$y_{e,k} = \hat{\mathbf{h}}_{e,k}^H \mathbf{x} + n_{e,k} = (\mathbf{h}_{ae,k}^H + \mathbf{h}_{re,k}^H \boldsymbol{\Phi} \mathbf{G}_{ar}) \mathbf{x} + n_{e,k}, \forall k \in \mathcal{K}, \quad (1b)$$

where the channels of the Alice-Bob link, IRS-Bob link and Alice-IRS link are denoted by  $\mathbf{h}_{ab} \in \mathbb{C}^{N_t \times 1}$ ,  $\mathbf{h}_{rb} \in \mathbb{C}^{M \times 1}$ , and  $\mathbf{G}_{ar} \in \mathbb{C}^{M \times N_t}$ , respectively, and  $\hat{\mathbf{h}}_b \triangleq \mathbf{h}_{ab} + \mathbf{G}_{ar}^H \boldsymbol{\Phi}^H \mathbf{h}_{rb}$ ,  $\hat{\mathbf{h}}_b \in \mathbb{C}^{N_t \times 1}$  is defined as the equivalent channel spanning from Alice to Bob. Similarly, the channels of the Alice-Eve link and IRS-Eve link are modeled by  $\mathbf{h}_{ae,k} \in \mathbb{C}^{N_t \times 1}$  and  $\mathbf{h}_{re,k} \in \mathbb{C}^{M \times 1}$ , respectively, and  $\hat{\mathbf{h}}_{e,k} = \mathbf{h}_{ae,k} + \mathbf{G}_{ar}^H \boldsymbol{\Phi}^H \mathbf{h}_{re,k}$ ,  $\hat{\mathbf{h}}_{e,k} \in \mathbb{C}^{N_t \times 1}$  is defined as the equivalent channel spanning from Alice to the  $k$ th Eve.  $n_b(t)$  is the additive white Gaussian noise (AWGN) at Bob, with zero mean and noise variance  $\sigma_b^2$ , i.e.,  $n_b \sim \mathcal{CN}(0, \sigma_b^2)$ .  $n_{e,k}$  is the AWGN at Eve with zero mean and noise covariance  $\sigma_{e,k}^2$ , i.e.,  $n_{e,k} \sim \mathcal{CN}(0, \sigma_{e,k}^2)$ . The phase shift coefficients of the IRS are collected in a diagonal matrix defined by  $\boldsymbol{\Phi} = \text{diag}\{\phi_1, \dots, \phi_m, \dots, \phi_M\}$ , where  $\phi_m = e^{j\theta_m}$ , and  $\theta_m \in [0, 2\pi)$  denotes the phase shift of the  $m$ -th reflecting element.

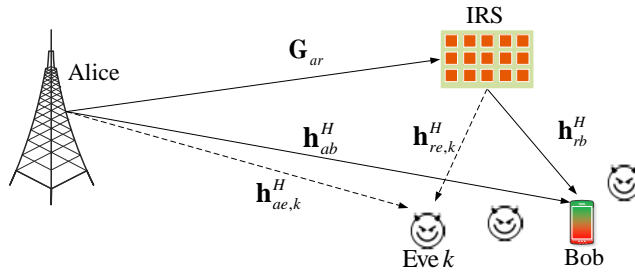


Fig. 1. An IRS-assisted secure communication system.

The transmit signal vector is

$$\mathbf{x} = \mathbf{s} + \mathbf{z} = \mathbf{w}\mathbf{s} + \mathbf{z}, \quad (2)$$

where  $\mathbf{s}$  is a data stream carrying the confidential information intended for Bob, and  $\mathbf{z}$  is the noise vector artificially created by Alice to interfere Eves, i.e., the so-called AN,  $\mathbf{w} \in \mathbb{C}^{N_t \times 1}$  is the beamforming vector of Alice. The confidential signal vector  $\mathbf{s}$  is assumed to follow a complex Gaussian distribution of  $\mathcal{CN}(\mathbf{0}, \mathbf{W})$ , where  $\mathbf{W} = \mathbf{w}\mathbf{w}^H$  is the transmit covariance matrix to be designed, and  $\text{rank}(\mathbf{W}) = 1$ . For the AN, we assume  $\mathbf{z}(t) \sim \mathcal{CN}(\mathbf{0}, \mathbf{Z})$ , where  $\mathbf{Z}$  is the AN covariance matrix to be designed.

The equivalent channel  $\hat{\mathbf{h}}_b$  and  $\hat{\mathbf{h}}_{e,k}$  can be respectively expressed in another way as

$$\hat{\mathbf{h}}_b^H = \mathbf{h}_{ab}^H + \boldsymbol{\phi}^T \text{diag}(\mathbf{h}_{rb}^H) \mathbf{G}_{ar} \triangleq \mathbf{h}_{ab}^H + \boldsymbol{\phi}^T \mathbf{G}_{cb}, \quad (3a)$$

$$\hat{\mathbf{h}}_{e,k}^H = \mathbf{h}_{ae,k}^H + \boldsymbol{\phi}^T \text{diag}(\mathbf{h}_{re,k}^H) \mathbf{G}_{ar} \triangleq \mathbf{h}_{ae,k}^H + \boldsymbol{\phi}^T \mathbf{G}_{ce,k}, \forall k \in \mathcal{K}, \quad (3b)$$

where  $\boldsymbol{\phi} = [\phi_1, \dots, \phi_m, \dots, \phi_M]^T$  is the phase shift vector.  $\mathbf{G}_{cb}$  is defined as  $\mathbf{G}_{cb} \triangleq \text{diag}(\mathbf{h}_{rb}^H) \mathbf{G}_{ar}$ ,  $\mathbf{G}_{cb} \in \mathbb{C}^{M \times N_t}$  denotes the cascaded channel from Alice to Bob via the IRS, and  $\mathbf{G}_{ce,k} = \text{diag}(\mathbf{h}_{re,k}^H) \mathbf{G}_{ar}$ ,  $\mathbf{G}_{ce,k} \in \mathbb{C}^{M \times N_t}$  denotes the cascaded channel from Alice to the  $k$ th Eve via the IRS.

The achievable data rate in (bit/s/Hz) of Bob  $C_b(\mathbf{W}, \mathbf{Z}, \boldsymbol{\Phi})$  is given as

$$C_b(\mathbf{W}, \mathbf{Z}, \boldsymbol{\Phi}) = \log \left( 1 + \frac{\hat{\mathbf{h}}_b^H \mathbf{W} \hat{\mathbf{h}}_b}{\sigma_b^2 + \hat{\mathbf{h}}_b^H \mathbf{Z} \hat{\mathbf{h}}_b} \right). \quad (4)$$

The achievable data rate in (bit/s/Hz) of the  $k$ th Eve  $C_{e,k}(\mathbf{W}, \mathbf{Z}, \boldsymbol{\Phi})$  is given as

$$C_{e,k}(\mathbf{W}, \mathbf{Z}, \boldsymbol{\Phi}) = \log \left( 1 + \frac{\hat{\mathbf{h}}_{e,k}^H \mathbf{W} \hat{\mathbf{h}}_{e,k}}{\sigma_{e,k}^2 + \hat{\mathbf{h}}_{e,k}^H \mathbf{Z} \hat{\mathbf{h}}_{e,k}} \right). \quad (5)$$

Then the achievable secrecy rate is

$$R_s(\mathbf{W}, \mathbf{Z}, \boldsymbol{\Phi}) = \min_{k \in \mathcal{K}} \{C_b(\mathbf{W}, \mathbf{Z}, \boldsymbol{\Phi}) - C_{e,k}(\mathbf{W}, \mathbf{Z}, \boldsymbol{\Phi})\}. \quad (6)$$

### B. Two CSI error Scenarios

We assume that Alice has imperfect CSI of Eves' links. There are two types of channels from Alice to Eves, which are the direct Alice-Eve channel  $\mathbf{h}_{ae,k}$  and the cascaded Alice-IRS-Eve channel  $\mathbf{G}_{ce,k}$ . We consider two scenarios of channel uncertainties next.

1) *Scenario 1: Partial CSI error:* Due to the passive features of the IRS, the CSI of the Alice-IRS-Eve link at the transmitter is much more challenging to obtain than the CSI of the Alice-Eve link at the transmitter. Hence, in this scenario, we assume the direct channel  $\mathbf{h}_{ae,k}$  is perfect, while the cascaded channel  $\mathbf{G}_{ce,k}$  is imperfect. The cascaded Alice-IRS-Eve channel can be represented as

$$\mathbf{G}_{ce,k} = \bar{\mathbf{G}}_{ce,k} + \Delta\mathbf{G}_{ce,k}, \forall k \in \mathcal{K}, \quad (7)$$

where  $\bar{\mathbf{G}}_{ce,k}$  is the estimated value of  $\mathbf{G}_{ce,k}$ , and  $\Delta\mathbf{G}_{ce,k}$  denotes the corresponding CSI error.

2) *Scenario 2: Full CSI errors:* In this scenario, we assume that both the direct channel  $\mathbf{h}_{ae,k}$  and the cascaded channel  $\mathbf{G}_{ce,k}$  are imperfect. In addition to the cascaded channel error model in (7), the direct channel  $\mathbf{h}_{ae,k}$  can be represented as

$$\mathbf{h}_{ae,k} = \bar{\mathbf{h}}_{ae,k} + \Delta\mathbf{h}_{ae,k}, \forall k \in \mathcal{K}, \quad (8)$$

where  $\bar{\mathbf{h}}_{ae,k}$  denotes the estimated value of channels  $\mathbf{h}_{ae,k}$  at Alice, and  $\Delta\mathbf{h}_{ae,k}$  is the unknown channel uncertainties.

In practice, the CSI is imperfect because of channel estimation and quantization errors. In this paper, we mainly consider the statistical CSI error model. The statistical CSI error model means that the CSI errors of  $\mathbf{h}_{ae,k}$  and  $\mathbf{G}_{ce,k}$  are random and follow certain distribution. Specifically, the CSI error vector is assumed to follow the CSCG distribution, i.e.,

$$\mathbf{g}_{he,k} \triangleq \Delta\mathbf{h}_{ae,k} \sim \mathcal{CN}(\mathbf{0}, \Sigma_{he,k}), \Sigma_{he,k} \succeq \mathbf{0}, \forall k \in \mathcal{K}, \quad (9a)$$

$$\mathbf{g}_{ge,k} \triangleq \text{vec}(\Delta\mathbf{G}_{ce,k}) \sim \mathcal{CN}(\mathbf{0}, \Sigma_{ge,k}), \Sigma_{ge,k} \succeq \mathbf{0}, \forall k \in \mathcal{K}, \quad (9b)$$

where  $\Sigma_{he,k} \in \mathbb{C}^{N_t \times N_t}$  and  $\Sigma_{ge,k} \in \mathbb{C}^{MN_t \times MN_t}$  are positive semidefinite covariance matrices of the CSI error. In addition,  $\mathbf{g}_{he,k}$  is independent of  $\mathbf{g}_{he,j}$  for any  $k \neq j$ , and  $\mathbf{g}_{ge,k}$  is independent of  $\mathbf{g}_{ge,j}$  for any  $k \neq j$ . Under these statistical CSI errors, we investigate the robust transmission design for the IRS-aided MISO secure communication system.

### III. THE OUTAGE CONSTRAINED ROBUST TRANSMISSION DESIGN

In this subsection, we consider a robust formulation where the CSI errors  $\Delta\mathbf{G}_{ce,k}$  and  $\Delta\mathbf{h}_{ae,k}$  are random and follow certain distribution. Specifically, the outage-constrained robust power minimization (OCR-PM) problem is investigated by jointly designing the transmit beamforming vector  $\mathbf{w}$ , the AN covariance matrix  $\mathbf{Z}$ , and the phase shifts matrix  $\Phi$  of the IRS, subject to the unit-modulus

constraints and the outage quality of service (QoS) constraints, ensuring that the achievable rate of the Bob should be above a threshold and the rate of the Eve to be below a threshold for all possible channel error realizations. In order to solve the non-convex robust design problem with probability constraints and coupled variables, an AO algorithm is proposed based on Bernstein-type inequality, SDR and penalty CCP [26].

#### A. Scenario 1: Partial CSI error

1) *Problem formulation:* Under the scenario of partial channel uncertainty, the direct channels  $\mathbf{h}_{ae,k}$  of the Alice-Eve link are perfect, and the cascaded channels  $\Delta \mathbf{G}_{ce,k}$  of the Alice-IRS-Eve link are imperfect. Then, the OCR-PM problem under the partial channel uncertainty can be formulated as

$$\min_{\mathbf{W}, \mathbf{Z}, \Phi} \text{Tr}(\mathbf{W} + \mathbf{Z}) \quad (10a)$$

$$\text{s.t. } C_b(\mathbf{W}, \mathbf{Z}, \Phi) \geq \log \gamma, \quad (10b)$$

$$\Pr_{\mathbf{g}_{ge,k}} \{C_{e,k}(\mathbf{W}, \mathbf{Z}, \Phi) \leq \log \beta\} \geq 1 - \rho_k, \forall k \in \mathcal{K}, \quad (10c)$$

$$\mathbf{Z} \succeq 0, \quad (10d)$$

$$\mathbf{W} \succeq 0, \quad (10e)$$

$$\text{rank}(\mathbf{W}) = 1, \quad (10f)$$

$$|\phi_m| = 1, m = 1, \dots, M, \quad (10g)$$

where  $\gamma \geq 1$  and  $\beta \geq 1$  are constant values, and  $\gamma \geq \beta$  is imposed to ensure a positive secrecy rate. The (10c) is the data rate constraint for Eves with outage probability limits.  $\rho_k \in (0, 1]$ ,  $k = 1, 2, \dots, K$  are the per-Eve secrecy outage probability. The rate outage constraint (10c) guarantees that the probability each Eve can decode at a data rate of no larger than  $\log \beta$  is no less than  $1 - \rho_k$ . By substituting (4) and (5) into (10), we can transform Problem (10) as

$$\min_{\mathbf{W}, \mathbf{Z}, \phi} \text{Tr}(\mathbf{W} + \mathbf{Z}) \quad (11a)$$

$$\text{s.t. } \hat{\mathbf{h}}_b^H [\mathbf{W} - (\gamma - 1)\mathbf{Z}] \hat{\mathbf{h}}_b \geq (\gamma - 1)\sigma_b^2, \quad (11b)$$

$$\Pr_{\mathbf{g}_{ge,k}} \left\{ \hat{\mathbf{h}}_{e,k}^H [\mathbf{W} - (\beta - 1)\mathbf{Z}] \hat{\mathbf{h}}_{e,k} \leq (\beta - 1)\sigma_{e,k}^2 \right\} \geq 1 - \rho_k, \forall k \in \mathcal{K}, \quad (11c)$$

$$(10d), (10e), (10f), (10g). \quad (11d)$$

The OCR-PM problem is computationally intractable due to the fact that the rate outage probability constraint (11c) has no simple closed-form expressions. To solve Problem (11), a safe approximation based on Bernstein-type inequality is given in the following lemma.

**Lemma 1:** (Bernstein-Type Inequality [31]) For any  $(\mathbf{A}, \mathbf{u}, c) \in \mathbb{H}^n \times \mathbb{C}^n \times \mathbb{R}$ ,  $\mathbf{v} \sim \mathcal{CN}(\mathbf{0}, \mathbf{I}_n)$  and  $\rho \in (0, 1]$ , the following implication holds:

$$\Pr_{\mathbf{v}} \{ \mathbf{v}^H \mathbf{A} \mathbf{v} + 2\text{Re}\{\mathbf{u}^H \mathbf{v}\} + c \geq 0 \} \geq 1 - \rho \quad (12)$$

$$\iff \text{Tr}(\mathbf{A}) - \sqrt{2 \ln(1/\rho)} \sqrt{\|\mathbf{A}\|_F^2 + 2\|\mathbf{u}\|^2} + \ln(\rho) \cdot \lambda^+(-\mathbf{A}) + c \geq 0 \quad (13)$$

$$\iff \begin{cases} \text{Tr}(\mathbf{A}) - \sqrt{-2 \ln(\rho)} \cdot x + \ln(\rho) \cdot y + c \geq 0, \\ \left\| \begin{bmatrix} \text{vec}(\mathbf{A}) \\ \sqrt{2}\mathbf{u} \end{bmatrix} \right\|_2 \leq x, \\ y\mathbf{I}_n + \mathbf{A} \succeq \mathbf{0}, y \geq 0 \end{cases} \quad (14)$$

where  $\lambda^+(\mathbf{A}) = \max(\lambda_{\max}(\mathbf{A}), 0)$ ,  $x$  and  $y$  are slack variables.

2) *Reformulation:* By substituting (7) into (11c), and defining  $\Xi_e \triangleq (\beta - 1)\mathbf{Z} - \mathbf{W}$  and  $\tilde{\sigma}_{e,k}^2 \triangleq (\beta - 1)\sigma_{e,k}^2$ , we have

$$\begin{aligned} & \Pr_{\mathbf{g}_{ge,k}} \left\{ \hat{\mathbf{h}}_{e,k}^H [\mathbf{W} - (\beta - 1)\mathbf{Z}] \hat{\mathbf{h}}_{e,k} \leq \tilde{\sigma}_{e,k}^2 \right\} \\ &= \Pr_{\mathbf{g}_{ge,k}} \left\{ [\mathbf{h}_{ae,k}^H + \phi^T (\bar{\mathbf{G}}_{ce,k} + \Delta \mathbf{G}_{ce,k})] \Xi_e [\mathbf{h}_{ae,k}^H + \phi^T (\bar{\mathbf{G}}_{ce,k} + \Delta \mathbf{G}_{ce,k})]^H + \tilde{\sigma}_{e,k}^2 \geq 0 \right\} \quad (15a) \end{aligned}$$

$$\begin{aligned} &= \Pr_{\mathbf{g}_{ge,k}} \left\{ \underbrace{\phi^T \Delta \mathbf{G}_{ce,k} \Xi_e \Delta \mathbf{G}_{ce,k}^H \phi^*}_{f_{1,k}^{\text{Partial}}} + 2\text{Re}\left\{ \underbrace{\phi^T \Delta \mathbf{G}_{ce,k} \Xi_e (\mathbf{h}_{ae,k} + \bar{\mathbf{G}}_{ce,k}^H \phi^*)}_{f_{2,k}^{\text{Partial}}} \right\} \right. \\ & \quad \left. + \underbrace{(\mathbf{h}_{ae,k}^H + \phi^T \bar{\mathbf{G}}_{ce,k}) \Xi_e (\mathbf{h}_{ae,k}^H + \phi^T \bar{\mathbf{G}}_{ce,k})^H}_{c_k^{\text{Partial}}} + \tilde{\sigma}_{e,k}^2 \geq 0 \right\}. \quad (15b) \end{aligned}$$

Let us equivalently represent the CSI error  $\mathbf{g}_{ge,k}$  as  $\mathbf{g}_{ge,k} = \Sigma_{ge,k}^{1/2} \mathbf{v}_{ge,k}$ , where  $\mathbf{v}_{ge,k} \sim \mathcal{CN}(\mathbf{0}, \mathbf{I}_{MN_t})$ , and  $\Sigma_{ge,k} = \Sigma_{ge,k}^{1/2} \Sigma_{ge,k}^{1/2}$ . Since  $\Sigma_{ge,k}$  is a semidefinite matrix, we have  $(\Sigma_{ge,k}^{1/2})^H = \Sigma_{ge,k}^{1/2}$  and

$(\Sigma_{ge,k}^{1/2})^T = (\Sigma_{ge,k}^{1/2})^*$ . The function  $f_{1,k}^{\text{Partial}}$  can be reformulated as

$$\begin{aligned}
f_{1,k}^{\text{Partial}} &= \text{Tr}(\Delta \mathbf{G}_{ce,k} \Xi_e \Delta \mathbf{G}_{ce,k}^H \phi^* \phi^T) \\
&\triangleq \text{Tr}(\Delta \mathbf{G}_{ce,k}^H \mathbf{E} \Delta \mathbf{G}_{ce,k} \Xi_e) \\
&\stackrel{(a)}{=} \text{vec}^H(\Delta \mathbf{G}_{ce,k})(\Xi_e^T \otimes \mathbf{E}) \text{vec}(\Delta \mathbf{G}_{ce,k}) \\
&= \mathbf{g}_{ge,k}^H (\Xi_e^T \otimes \mathbf{E}) \mathbf{g}_{ge,k} \\
&= \mathbf{v}_{ge,k}^H \Sigma_{ge,k}^{1/2} (\Xi_e^T \otimes \mathbf{E}) \Sigma_{ge,k}^{1/2} \mathbf{v}_{ge,k} \\
&\triangleq \mathbf{v}_{ge,k}^H \mathbf{A}_{e,k} \mathbf{v}_{ge,k}, \tag{16}
\end{aligned}$$

where  $\mathbf{E} \triangleq \phi^* \phi^T$ ,  $\mathbf{A}_{e,k} \triangleq \Sigma_{ge,k}^{1/2} (\Xi_e^T \otimes \mathbf{E}) \Sigma_{ge,k}^{1/2}$ , and (a) is obtained by invoking the identity  $\text{Tr}(\mathbf{A}^H \mathbf{B} \mathbf{C} \mathbf{D}) = \text{vec}^H(\mathbf{A})(\mathbf{D}^T \otimes \mathbf{B}) \text{vec}(\mathbf{C})$ . The function  $f_{2,k}^{\text{Partial}}$  can then be reformulated as

$$\begin{aligned}
f_{2,k}^{\text{Partial}} &= \text{Tr}(\Delta \mathbf{G}_{ce,k} \Xi_e (\mathbf{h}_{ae,k} + \bar{\mathbf{G}}_{ce,k}^H \phi^*) \phi^T) \\
&= \text{Tr}(\Delta \mathbf{G}_{ce,k} \Xi_e (\mathbf{h}_{ae,k} \phi^T + \bar{\mathbf{G}}_{ce,k}^H \mathbf{E})) \\
&\stackrel{(b)}{=} \text{vec}^H(\phi^* \mathbf{h}_{ae,k}^H + \mathbf{E} \bar{\mathbf{G}}_{ce,k})(\Xi_e^T \otimes \mathbf{I}_M) \text{vec}(\Delta \mathbf{G}_{ce,k}) \\
&= \text{vec}^H(\phi^* \mathbf{h}_{ae,k}^H + \mathbf{E} \bar{\mathbf{G}}_{ce,k})(\Xi_e^T \otimes \mathbf{I}_M) \mathbf{g}_{ge,k} \\
&= \text{vec}^H(\phi^* \mathbf{h}_{ae,k}^H + \mathbf{E} \bar{\mathbf{G}}_{ce,k})(\Xi_e^T \otimes \mathbf{I}_M) \Sigma_{ge,k}^{1/2} \mathbf{v}_{ge,k} \\
&\triangleq \mathbf{u}_{e,k}^H \mathbf{v}_{ge,k}, \tag{17}
\end{aligned}$$

where  $\mathbf{u}_{e,k} \triangleq \Sigma_{ge,k}^{1/2} (\Xi_e^* \otimes \mathbf{I}_M) \text{vec}(\phi^* \mathbf{h}_{ae,k}^H + \mathbf{E} \bar{\mathbf{G}}_{ce,k})$ , and the (b) is obtained by invoking the identity  $\text{Tr}(\mathbf{A} \mathbf{B} \mathbf{C}^H) = \text{vec}^H(\mathbf{C})(\mathbf{B}^T \otimes \mathbf{I}) \text{vec}(\mathbf{A})$ .

By substituting (16) and (17) into (15b), the leakage data rate outage constraints (11c) for Eves become

$$(11c) \Leftrightarrow \Pr_{\mathbf{v}_{ce,k}} \left\{ \mathbf{v}_{ge,k}^H \mathbf{A}_{e,k} \mathbf{v}_{ge,k} + 2 \text{Re} \{ \mathbf{u}_{e,k}^H \mathbf{v}_{ge,k} \} + c_k^{\text{Partial}} \geq 0 \right\} \geq 1 - \rho_k, \forall k \in \mathcal{K}. \tag{18}$$

The equivalence in (18) implies that the outage probability in (11c) can be characterized by the quadratic inequality w.r.t. the Gaussian random vector  $\mathbf{v}_{ge,k}$ . By invoking Lemma 1 and introducing the slack variables  $\mathbf{x} = [x_1, x_2, \dots, x_K]^T$ , and  $\mathbf{y} = [y_1, y_2, \dots, y_K]^T$ , we arrive at the desired safe

approximation of OCR-PM, which is shown as

$$\min_{\mathbf{W}, \mathbf{Z}, \phi, \mathbf{A}_e, \mathbf{x}, \mathbf{y}} \text{Tr}(\mathbf{W} + \mathbf{Z}) \quad (19a)$$

$$\text{s.t.} \quad \text{Tr}(\mathbf{A}_{e,k}) - \sqrt{-2 \ln(\rho_k)} \cdot x_k + \ln(\rho_k) \cdot y_k + c_k^{\text{Partial}} \geq 0, \quad (19b)$$

$$\left\| \begin{bmatrix} \text{vec}(\mathbf{A}_{e,k}) \\ \sqrt{2} \mathbf{u}_{e,k} \end{bmatrix} \right\|_2 \leq x_k, \quad (19c)$$

$$y_k \mathbf{I}_{MN_t} + \mathbf{A}_{e,k} \succeq \mathbf{0}, y_k \geq 0, \quad (19d)$$

$$(11b), (10d), (10e), (10f), (10g), \quad (19e)$$

where  $\mathbf{A}_e = [\mathbf{A}_{e,1}, \mathbf{A}_{e,2}, \dots, \mathbf{A}_{e,K}]$ . The constraints in Problem (19) can be further simplified by some mathematical transformations as follows:

$$\begin{aligned} \|\text{vec}(\mathbf{A}_{e,k})\|^2 &= \|\mathbf{A}_{e,k}\|_F^2 = \text{Tr}[\mathbf{A}_{e,k} \mathbf{A}_{e,k}^H] = \text{Tr}[\Sigma_{ge,k}^{1/2} (\Xi_e^T \otimes \mathbf{E}) \Sigma_{ge,k}^{1/2} \Sigma_{ge,k}^{1/2} (\Xi_e^* \otimes \mathbf{E}^H) \Sigma_{ge,k}^{1/2}] \\ &= \text{Tr}[(\Xi_e^T \otimes \mathbf{E})^H \Sigma_{ge,k} (\Xi_e^T \otimes \mathbf{E}) \Sigma_{ge,k}] \\ &\stackrel{(c)}{=} \text{vec}^H(\Xi_e^T \otimes \mathbf{E}) (\Sigma_{ge,k}^T \otimes \Sigma_{ge,k}) \text{vec}(\Xi_e^T \otimes \mathbf{E}) \\ &= \text{vec}^H(\Xi_e^T \otimes \mathbf{E}) [(\Sigma_{ge,k}^{1/2T} \Sigma_{ge,k}^{1/2T}) \otimes (\Sigma_{ge,k}^{1/2} \Sigma_{ge,k}^{1/2})] \text{vec}(\Xi_e^T \otimes \mathbf{E}) \\ &= \text{vec}^H(\Xi_e^T \otimes \mathbf{E}) [(\Sigma_{ge,k}^{1/2T} \otimes \Sigma_{ge,k}^{1/2})^H (\Sigma_{ge,k}^{1/2T} \otimes \Sigma_{ge,k}^{1/2})] \text{vec}(\Xi_e^T \otimes \mathbf{E}) \\ &= \left\| (\Sigma_{ge,k}^{1/2T} \otimes \Sigma_{ge,k}^{1/2}) \text{vec}(\Xi_e^T \otimes \mathbf{E}) \right\|^2. \end{aligned} \quad (20)$$

where (c) is obtained by invoking the identity  $\text{Tr}(\mathbf{A}^H \mathbf{B} \mathbf{C} \mathbf{D}) = \text{vec}^H(\mathbf{A})(\mathbf{D}^T \otimes \mathbf{B}) \text{vec}(\mathbf{C})$ . Obviously, when  $\phi$  is fixed, the  $c_k^{\text{Partial}}$ ,  $\text{Tr}(\mathbf{A}_k)$ ,  $\|\text{vec}(\mathbf{A}_k)\|^2$  and  $\|\mathbf{u}_{ce,k}\|$  are all convex functions of  $\Xi_e$  (also  $\mathbf{W}$  and  $\mathbf{Z}$ ). By substituting the expressions of (20) into (19), the OCR-PM Problem in (19) can be recast as

$$\min_{\mathbf{W}, \mathbf{Z}, \phi, \mathbf{x}, \mathbf{y}} \text{Tr}(\mathbf{W} + \mathbf{Z}) \quad (21a)$$

$$\text{s.t.} \quad \text{Tr}(\Sigma_{ge,k}^{1/2} (\Xi_e^T \otimes \mathbf{E}) \Sigma_{ge,k}^{1/2}) - \sqrt{-2 \ln(\rho_k)} \cdot x_k + \ln(\rho_k) \cdot y_k + c_k^{\text{Partial}} \geq 0, \quad (21b)$$

$$\left\| \begin{bmatrix} (\Sigma_{ge,k}^{1/2T} \otimes \Sigma_{ge,k}^{1/2}) \text{vec}(\Xi_e^T \otimes \mathbf{E}) \\ \sqrt{2} \Sigma_{ge,k}^{1/2} (\Xi_e^* \otimes \mathbf{I}_M) \text{vec}(\phi^* \mathbf{h}_{ae,k}^H + \mathbf{E} \tilde{\mathbf{G}}_{ce,k}) \end{bmatrix} \right\|_2 \leq x_k, \quad (21c)$$

$$y_k \mathbf{I}_{MN_t} + \Sigma_{ge,k}^{1/2} (\Xi_e^T \otimes \mathbf{E}) \Sigma_{ge,k}^{1/2} \succeq \mathbf{0}, y_k \geq 0, \quad (21d)$$

$$(11b), (10d), (10e), (10f), (10g). \quad (21e)$$

3) *Solving the beamforming matrix and AN covariance matrix:* The above Problem (21) is not convex due to the coupled  $\Xi_e$  and  $\phi$ . To solve it, we use the AO method to update  $\{\mathbf{W}, \mathbf{Z}, \mathbf{x}, \mathbf{y}\}$  and  $\phi$  alternately. Specifically, when  $\phi$  is fixed, Problem (21) becomes convex w.r.t.  $\{\mathbf{W}, \mathbf{Z}, \mathbf{x}, \mathbf{y}\}$  if the rank one constraint in (10f) is relaxed. By using the SDR technique, the optimization problem w.r.t.  $\{\mathbf{W}, \mathbf{Z}, \mathbf{x}, \mathbf{y}\}$  becomes

$$\min_{\mathbf{W}, \mathbf{Z}, \mathbf{x}, \mathbf{y}} \text{Tr}(\mathbf{W} + \mathbf{Z}) \quad (22a)$$

$$\text{s.t.} \quad (21b), (21c), (21d), \quad (22b)$$

$$(11b), (10d), (10e). \quad (22c)$$

Problem (22) is convex, and can be solved by the CVX toolbox. Due to the application of SDR, the obtained  $\mathbf{W}$  of Problem (22) may not be a rank-one solution. If not, the suboptimal beamforming vector can be obtained by using the Gaussian randomization method.

4) *Solving the phase shifts of the IRS:* When  $\{\mathbf{W}, \mathbf{Z}, \mathbf{x}, \mathbf{y}\}$  are fixed, Problem (21) becomes a feasibility check problem. In order to improve the converged solution in the optimization process, the data rate inequalities for Bob in (11b) and Eves in (15a) can be modified by introducing slack variables, and recast as

$$\hat{\mathbf{h}}_b^H [\mathbf{W} - (\gamma - 1)\mathbf{Z}] \hat{\mathbf{h}}_b \geq \tilde{\sigma}_b^2 + \delta_0, \delta_0 \geq 0, \quad (23a)$$

$$[\mathbf{h}_{ae,k}^H + \phi^T (\bar{\mathbf{G}}_{ce,k} + \Delta \mathbf{G}_{ce,k})] \Xi_e [\mathbf{h}_{ae,k}^H + \phi^T (\bar{\mathbf{G}}_{ce,k} + \Delta \mathbf{G}_{ce,k})]^H + \tilde{\sigma}_{e,k}^2 - \delta_k \geq 0, \delta_k \geq 0. \quad (23b)$$

where  $\tilde{\sigma}_b^2 \triangleq (\gamma - 1)\sigma_b^2$ .

Then, by fixing  $\mathbf{W}$  and  $\mathbf{Z}$  obtained in the last iteration, and using the BTI for the outage probability constraint of the leaked data rate again, the optimization problem w.r.t.  $\phi, \delta, \mathbf{x}, \mathbf{y}$  becomes

$$\max_{\phi, \delta, \mathbf{x}, \mathbf{y}} \sum_{k=0}^K \delta_k \quad (24a)$$

$$\text{s.t.} \quad \text{Tr}(\Sigma_{ge,k}^{1/2} (\Xi_e^T \otimes \mathbf{E}) \Sigma_{ge,k}^{1/2}) - \sqrt{-2 \ln(\rho_k)} \cdot x_k + \ln(\rho_k) \cdot y_k + c_k^{\text{Partial}} - \delta_k \geq 0, \quad (24b)$$

$$(21c), (21d), (10g), \quad (24c)$$

$$\hat{\mathbf{h}}_b^H [\mathbf{W} - (\gamma - 1)\mathbf{Z}] \hat{\mathbf{h}}_b \geq \tilde{\sigma}_b^2 + \delta_0, \quad (24d)$$

$$\delta \geq \mathbf{0}, \quad (24e)$$

where  $\delta = [\delta_0, \delta_1, \delta_2, \dots, \delta_K]^T$ .

The difficulty for solving Problem (24) lies in checking the convexity of the constraints. To transform it into a convex problem, some mathematical manipulations on these constraints are performed by four steps as follows.

**Step 1:** Transform the constraint of (24b) into convex ones.

(1) We note that the  $c_k^{\text{Partial}}$  in (24b) is non-concave w.r.t.  $\phi$  due to the fact that  $\bar{\mathbf{G}}_{ce,k} \bar{\Xi}_e \bar{\mathbf{G}}_{ce,k}^H$  is a non-negative semidefinite matrix. To address this issue, the term  $c_k^{\text{Partial}}$  can be equivalently rewritten as

$$\begin{aligned} c_k^{\text{Partial}}(\phi) &= (\mathbf{h}_{ae,k}^H + \phi^T \bar{\mathbf{G}}_{ce,k}) \bar{\Xi}_e (\mathbf{h}_{ae,k}^H + \phi^T \bar{\mathbf{G}}_{ce,k})^H + (\beta - 1) \sigma_{e,k}^2 - \phi^T c_{c,k} \mathbf{I}_M \phi^* + M c_{c,k} \\ &= \phi^T (\bar{\mathbf{G}}_{ce,k} \bar{\Xi}_e \bar{\mathbf{G}}_{ce,k}^H - c_{c,k} \mathbf{I}_M) \phi^* + 2 \text{Re} \{ \phi^T \bar{\mathbf{G}}_{ce,k} \bar{\Xi}_e \mathbf{h}_{ae,k} \} + \mathbf{h}_{ae,k}^H \bar{\Xi}_e \mathbf{h}_{ae,k} \\ &\quad + M c_{c,k} + \tilde{\sigma}_{e,k}^2, \end{aligned} \quad (25)$$

where the unit-modulus property  $\phi^T \phi^* = M$  is utilized.  $c_{c,k}$  is chosen as  $c_{c,k} = \lambda_{\max} \{ \bar{\mathbf{G}}_{ce,k} (\beta - 1) \mathbf{Z} \bar{\mathbf{G}}_{ce,k}^H \}$ . Since  $\bar{\Xi}_e = (\beta - 1) \mathbf{Z} - \mathbf{W}$ , we have  $\bar{\mathbf{G}}_{ce,k} \bar{\Xi}_e \bar{\mathbf{G}}_{ce,k}^H - c_{c,k} \mathbf{I}_M \preceq \mathbf{0}$ , and the expression of  $c_k^{\text{Partial}}(\phi)$  in (25) becomes concave w.r.t.  $\phi$ .

(2) The term  $\text{Tr}(\Sigma_{ge,k}^{1/2} (\bar{\Xi}_e^T \otimes \mathbf{E}) \Sigma_{ge,k}^{1/2})$  in (24b) can be rewritten as

$$\begin{aligned} \text{Tr}(\Sigma_{ge,k}^{1/2} (\bar{\Xi}_e^T \otimes \mathbf{E}) \Sigma_{ge,k}^{1/2}) &\stackrel{(d)}{=} \text{vec}^H(\Sigma_{ge,k}^{1/2}) (\mathbf{I}_{MN_t} \otimes (\bar{\Xi}_e^T \otimes \mathbf{E})) \text{vec}(\Sigma_{ge,k}^{1/2}) \\ &= \text{vec}^H(\Sigma_{ge,k}^{1/2}) (\mathbf{I}_{MN_t} \otimes (\bar{\Xi}_e^T \otimes (\phi^* \phi^T))) \text{vec}(\Sigma_{ge,k}^{1/2}) \\ &= \text{vec}^H(\Sigma_{gx,k}) (\mathbf{I}_{MN_t} \otimes \bar{\Xi}_e^T \otimes (\phi^* \phi^T)) \text{vec}(\Sigma_{gx,k}) \\ &\stackrel{(e)}{=} \phi^T \Sigma_{gx,k} (\mathbf{I}_{MN_t} \otimes \bar{\Xi}_e) \Sigma_{gx,k}^H \phi^*, \end{aligned} \quad (26)$$

where (d) is obtained by invoking  $\text{Tr}(\mathbf{A}^H \mathbf{B} \mathbf{C} \mathbf{D}) = \text{vec}^H(\mathbf{A}) (\mathbf{D}^T \otimes \mathbf{B}) \text{vec}(\mathbf{C})$ , (e) is obtained by invoking the identity  $\text{vec}(\mathbf{X})^H (\mathbf{B}^T \otimes \mathbf{c} \mathbf{a}^H) \text{vec}(\mathbf{X}) = \mathbf{a}^H \mathbf{X} \mathbf{B} \mathbf{X}^H \mathbf{c}$ , in which  $\mathbf{B}^T = \mathbf{I}_{MN_t} \otimes \bar{\Xi}_e^T$ ,  $\mathbf{c} = \phi^*$ ,  $\mathbf{a}^H = \phi^T$ , and  $\mathbf{X} = \Sigma_{gx,k}$ . When using this identity, the matrix dimension must be matched. Thus,  $\Sigma_{gx,k} \in \mathbb{C}^{M \times MN_t^2}$  is obtained by remapping the column vector  $\text{vec}(\Sigma_{ge,k}^{1/2}) \in \mathbb{C}^{(MN_t)^2 \times 1}$  into an  $M \times MN_t^2$  dimensional matrix, which can be expressed as  $\Sigma_{gx,k} = \text{unvec}[\text{vec}(\Sigma_{ge,k}^{1/2})]$ .

It is also noted that (26) is also non-concave w.r.t.  $\phi$  since  $\bar{\Xi}_e = (\beta - 1) \mathbf{Z} - \mathbf{W}$ . Similarly, we reformulate (26) into a concave form as

$$\text{Tr}(\Sigma_{ge,k}^{1/2} (\bar{\Xi}_e^T \otimes \mathbf{E}) \Sigma_{ge,k}^{1/2}) = \phi^T [\Sigma_{gx,k} (\mathbf{I}_{MN_t} \otimes \bar{\Xi}_e) \Sigma_{gx,k}^H - c_{t,k} \mathbf{I}_M] \phi^* + M c_{t,k}, \quad (27)$$

where  $c_{t,k} = \lambda_{\max} \{ \Sigma_{gx,k} (\mathbf{I}_{MN_t} \otimes ((\beta - 1) \mathbf{Z})) \Sigma_{gx,k}^H \}$ .

(3) By substituting (25) and (27) into (24b), we have the following convex constraint:

$$(24b) \Leftrightarrow c_{tc,k}^{\text{partial}}(\boldsymbol{\phi}) \geq 0 \quad (28)$$

where

$$\begin{aligned} c_{tc,k}^{\text{partial}}(\boldsymbol{\phi}) &\triangleq \boldsymbol{\phi}^T [\boldsymbol{\Sigma}_{gx,k} (\mathbf{I}_{MN_t} \otimes \boldsymbol{\Xi}_e) \boldsymbol{\Sigma}_{gx,k}^H - c_{t,k} \mathbf{I}_M] \boldsymbol{\phi}^* + M c_{t,k} - \sqrt{-2 \ln(\rho_k)} \cdot x_k + \ln(\rho_k) \cdot y_k \\ &\quad + \boldsymbol{\phi}^T (\bar{\mathbf{G}}_{ce,k} \boldsymbol{\Xi}_e \bar{\mathbf{G}}_{ce,k}^H - c_{c,k} \mathbf{I}_M) \boldsymbol{\phi}^* + 2 \text{Re} \{ \boldsymbol{\phi}^T \bar{\mathbf{G}}_{ce,k} \boldsymbol{\Xi}_e \mathbf{h}_{ae,k} \} + \mathbf{h}_{ae,k}^H \boldsymbol{\Xi}_e \mathbf{h}_{ae,k} \\ &\quad + M c_{c,k} + \tilde{\sigma}_{e,k}^2 - \delta_k. \end{aligned} \quad (29)$$

As a result, the non-convex constraint in (24b) is transformed into a convex one in (28).

**Step 2:** Transform the constraint in (21c) to be convex.

(1) In constraint (21c), we can find an upper bound of  $(\boldsymbol{\Sigma}_{ge,k}^{1/2T} \otimes \boldsymbol{\Sigma}_{ge,k}^{1/2}) \text{vec}(\boldsymbol{\Xi}_e^T \otimes \mathbf{E})$  as

$$\left\| (\boldsymbol{\Sigma}_{ge,k}^{1/2T} \otimes \boldsymbol{\Sigma}_{ge,k}^{1/2}) \text{vec}(\boldsymbol{\Xi}_e^T \otimes \mathbf{E}) \right\| \stackrel{(f)}{\leq} \left\| (\boldsymbol{\Sigma}_{ge,k}^{1/2T} \otimes \boldsymbol{\Sigma}_{ge,k}^{1/2}) \right\|_2 \left\| \text{vec}(\boldsymbol{\Xi}_e^T \otimes \mathbf{E}) \right\|_2, \quad (30a)$$

$$\Leftrightarrow \stackrel{(g)}{\leq} \lambda_{\max}(\boldsymbol{\Sigma}_{ge,k}^{1/2T} \otimes \boldsymbol{\Sigma}_{ge,k}^{1/2}) M \|\boldsymbol{\Xi}_e\|_F, \quad (30b)$$

where the step (f) is obtained due to  $\|\mathbf{A}\mathbf{x}\|_2 \leq \|\mathbf{A}\|_2 \|\mathbf{x}\|_2$ ,  $\|\mathbf{A}\|_2 = \sigma_{\max}\{\mathbf{A}\}$  denotes the spectral norm of matrix  $\mathbf{A}$ , and  $\sigma_{\max}\{\mathbf{A}\}$  represents the maximum singular value of  $\mathbf{A}$ . The equality  $\|\mathbf{A}\mathbf{x}\|_2 = \|\mathbf{A}\|_2 \|\mathbf{x}\|_2$  is satisfied when the matrix  $\mathbf{A}$  is an unitary matrix. The step (g) is obtained due to  $\sigma_{\max}\{\mathbf{A}\} = \lambda_{\max}\{\mathbf{A}\}$  if  $\mathbf{A} \in \mathbb{H}^n$ , where  $\lambda_{\max}\{\mathbf{A}\}$  denotes the maximum eigen value of matrix  $\mathbf{A}$ , and the following property:

$$\begin{aligned} \left\| \text{vec}(\boldsymbol{\Xi}_e^T \otimes \mathbf{E}) \right\|^2 &= \text{Tr}[(\boldsymbol{\Xi}_e^T \otimes \mathbf{E})(\boldsymbol{\Xi}_e^* \otimes \mathbf{E})] = \text{Tr}[(\boldsymbol{\Xi}_e^T \boldsymbol{\Xi}_e^*) \otimes (\mathbf{E}\mathbf{E})] \\ &= \text{Tr}[(\boldsymbol{\Xi}_e^T \boldsymbol{\Xi}_e^*)] \text{Tr}[(\mathbf{E}\mathbf{E})] = M^2 \|\boldsymbol{\Xi}_e\|_F^2. \end{aligned} \quad (31)$$

It is observed that when  $\boldsymbol{\Sigma}_{ge,k} = \mathbf{I}_{MN_t}$ , the inequality in (30b) holds with equality.

(2) In constraint (21c), we can find an upper bound of  $\boldsymbol{\Sigma}_{ge,k}^{1/2} (\boldsymbol{\Xi}_e^* \otimes \mathbf{I}_M) \text{vec}(\boldsymbol{\phi}^* \mathbf{h}_{ae,k}^H + \mathbf{E} \bar{\mathbf{G}}_{ce,k})$  as

$$\left\| \boldsymbol{\Sigma}_{ge,k}^{1/2} (\boldsymbol{\Xi}_e^* \otimes \mathbf{I}_M) \text{vec}[\boldsymbol{\phi}^* (\mathbf{h}_{ae,k}^H + \boldsymbol{\phi}^T \bar{\mathbf{G}}_{ce,k})] \right\| \stackrel{(h)}{\leq} \lambda_{\max}(\boldsymbol{\Sigma}_{ge,k}^{1/2} (\boldsymbol{\Xi}_e^* \otimes \mathbf{I}_M)) \left\| (\mathbf{h}_{ae,k}^* + \bar{\mathbf{G}}_{ce,k}^T \boldsymbol{\phi}) \otimes \boldsymbol{\phi}^* \right\|, \quad (32a)$$

$$\stackrel{(i)}{=} \lambda_{\max}(\boldsymbol{\Sigma}_{ge,k}^{1/2} (\boldsymbol{\Xi}_e^* \otimes \mathbf{I}_M)) \sqrt{M} \left\| (\mathbf{h}_{ae,k}^* + \bar{\mathbf{G}}_{ce,k}^T \boldsymbol{\phi}) \right\|, \quad (32b)$$

where (h) is obtained due to  $\|\mathbf{A}\mathbf{x}\|_2 \leq \|\mathbf{A}\|_2 \|\mathbf{x}\|_2$  and  $\text{vec}(\mathbf{a}\mathbf{b}^T) = \mathbf{b} \otimes \mathbf{a}$ . The step in (i) is obtained by using Lemma 2 as follows.

**Lemma 2:** For any two vectors  $\mathbf{b}$  and  $\mathbf{c}$ , we have  $\|\mathbf{b} \otimes \mathbf{c}\| = \|\mathbf{b}\| \|\mathbf{c}\|$ . In particular, we have  $\|\mathbf{a} \otimes \mathbf{a}\| = \mathbf{a}^H \mathbf{a}$ .

**Proof:** Please refer to Appendix C. ■

It is observed that when  $\Sigma_{ge,k} = \mathbf{I}_{MN_t}$ , the inequality in (32b) becomes an equality.

Finally, by utilizing the upper bounds in (30b) and (32b), the constraint in (21c) becomes convex as

$$(21c) \Leftrightarrow \left\| \begin{array}{c} \lambda_{\max}(\Sigma_{ge,k}^{1/2T} \otimes \Sigma_{ge,k}^{1/2}) M \text{vec}(\Xi_e) \\ \sqrt{2M} \lambda_{\max}(\Sigma_{ge,k}^{1/2} (\Xi_e^* \otimes \mathbf{I}_M)) (\mathbf{h}_{ae,k}^* + \bar{\mathbf{G}}_{ce,k}^T \phi) \end{array} \right\| \leq x_k. \quad (33)$$

**Step 3:** Transform the constraint of (21d) to be convex.

Since  $\beta \geq 1$ , we note that  $c_g = \lambda_{\max}\{(\beta - 1)\mathbf{Z}\} \geq 0$ . By substituting  $\Xi_e = (\beta - 1)\mathbf{Z} - \mathbf{W}$  into (21d), and adding  $\Sigma_{ge,k}^{1/2} ((c_g \mathbf{I}_{N_t})^T \otimes \mathbf{E}) \Sigma_{ge,k}^{1/2}$  on both sides of (21d), we have

$$(21d) \Leftrightarrow y_k \mathbf{I}_{N_t M} + \Sigma_{ge,k}^{1/2} ((c_g \mathbf{I}_{N_t})^T \otimes \mathbf{E}) \Sigma_{ge,k}^{1/2} \succeq \Sigma_{ge,k}^{1/2} (\mathbf{W}^T \otimes \mathbf{E}) \Sigma_{ge,k}^{1/2} + \Sigma_{ge,k}^{1/2} [(c_g \mathbf{I}_{N_t} - (\beta - 1)\mathbf{Z})^T \otimes \mathbf{E}] \Sigma_{ge,k}^{1/2} \quad (34a)$$

$$\Leftrightarrow y_k \mathbf{I}_{N_t M} + \Sigma_{ge,k}^{1/2} ((c_g \mathbf{I}_{N_t})^T \otimes \mathbf{E}) \Sigma_{ge,k}^{1/2} \succeq \Sigma_{ge,k}^{1/2} [(\mathbf{W} + \mathbf{Z}_g)^T \otimes \mathbf{E}] \Sigma_{ge,k}^{1/2} \quad (34b)$$

$$\Leftrightarrow y_k + \lambda_{\min}\{\Sigma_{ge,k}^{1/2} ((c_g \mathbf{I}_{N_t})^T \otimes \mathbf{E}) \Sigma_{ge,k}^{1/2}\} \geq \lambda_{\max}\{\Sigma_{ge,k}^{1/2} (\mathbf{V}_{wgz}^* \otimes \phi^*) (\mathbf{V}_{wgz}^T \otimes \phi^T) \Sigma_{ge,k}^{1/2}\} \quad (34c)$$

$$\Leftrightarrow y_k \stackrel{(j)}{\geq} \left\| \Sigma_{ge,k}^{1/2} (\mathbf{V}_{wgz}^* \otimes \phi^*) \right\|_2^2, \quad (34d)$$

where  $\mathbf{Z}_g \triangleq c_g \mathbf{I}_{N_t} - (\beta - 1)\mathbf{Z}$ ,  $\mathbf{W} + \mathbf{Z}_g \triangleq \mathbf{V}_{wgz} \mathbf{V}_{wgz}^H$ ,  $\mathbf{Z}_g \succeq \mathbf{0}$  and  $\mathbf{W} + \mathbf{Z}_g \succeq \mathbf{0}$ . The step in (j) is obtained because  $\lambda_{\min}\{\Sigma_{ge,k}^{1/2} ((c_g \mathbf{I}_{N_t})^T \otimes \mathbf{E}) \Sigma_{ge,k}^{1/2}\} = 0$ , and the proof is given in Appendix A. The constraint (34d) is convex, and can be equivalently written as

$$(21d) \Leftrightarrow \left\| (\Sigma_{ge,k}^{1/2} (\mathbf{V}_{wgz}^* \otimes \phi^*)) \right\|_2 - \sqrt{(y_k)} \leq 0, y_k \geq 0, \quad (35)$$

which is convex.

**Step 4:** Transform the constraint of (24d) to be convex.

By substituting (3a) into the data rate requirement for Bob in (24d), and defining  $\Xi_b \triangleq (\gamma - 1)\mathbf{Z} - \mathbf{W}$ , the constraint (24d) can be recast as

$$(24d) \Leftrightarrow (\mathbf{h}_{ab}^H + \phi^T \mathbf{G}_{cb}) [\mathbf{W} - (\gamma - 1)\mathbf{Z}] (\mathbf{h}_{ab} + \mathbf{G}_{cb}^H \phi^*) \geq \tilde{\sigma}_b^2 + \delta_0, \quad (36a)$$

$$\begin{aligned} &\Leftrightarrow \phi^T \mathbf{G}_{cb} \Xi_b \mathbf{G}_{cb}^H \phi^* + \mathbf{h}_{ab}^H \Xi_b \mathbf{G}_{cb}^H \phi^* + \phi^T \mathbf{G}_{cb} \Xi_b \mathbf{h}_{ab} \\ &\quad + \mathbf{h}_{ab}^H \Xi_b \mathbf{h}_{ab} + \tilde{\sigma}_b^2 + \delta_0 \leq 0. \end{aligned} \quad (36b)$$

To build the convexity of (36b), it is reformulated as

$$(24d) \Leftrightarrow \phi^T [\mathbf{G}_{cb} \mathbf{\Xi}_b \mathbf{G}_{cb}^H - c_b \mathbf{I}_M] \phi^* + \mathbf{h}_{ab}^H \mathbf{\Xi}_b \mathbf{G}_{cb}^H \phi^* + \phi^T \mathbf{G}_{cb} \mathbf{\Xi}_b \mathbf{h}_{ab} + \mathbf{h}_{ab}^H \mathbf{\Xi}_b \mathbf{h}_{ab} + \tilde{\sigma}_b^2 + \delta_0 \leq -M c_b, \quad (37)$$

$$\Leftrightarrow b(\phi) \leq 0, \quad (38)$$

where  $c_b = \lambda_{\min}\{\mathbf{G}_{cb} \mathbf{\Xi}_b \mathbf{G}_{cb}^H\}$ ,  $\lambda_{\min}\{\mathbf{A}\}$  denotes the minimum eigenvalue of the matrix  $\mathbf{A}$ , and

$$b(\phi) \triangleq \phi^T [\mathbf{G}_{cb} \mathbf{\Xi}_b \mathbf{G}_{cb}^H - c_b \mathbf{I}_M] \phi^* + \mathbf{h}_{ab}^H \mathbf{\Xi}_b \mathbf{G}_{cb}^H \phi^* + \phi^T \mathbf{G}_{cb} \mathbf{\Xi}_b \mathbf{h}_{ab} + \mathbf{h}_{ab}^H \mathbf{\Xi}_b \mathbf{h}_{ab} + \tilde{\sigma}_b^2 + \delta_0 + M c_b. \quad (39)$$

Finally, based on the mathematical manipulations of Steps 1-4 above, Problem (24) can be reformulated as

$$\max_{\phi, \delta, \mathbf{x}, \mathbf{y}} \sum_{k=0}^K \delta_k \quad (40a)$$

$$\text{s.t. (28), (33), (35), (38), (24e),} \quad (40b)$$

$$|\phi_m| = 1, m = 1, \dots, M. \quad (40c)$$

The only nonconvex constraint in Problem (40) is the unit-modulus constraint. To deal with it, the penalty CCP method is utilized. The constraint of (40c) is equivalent to  $|\phi_m|^2 \leq 1$  and  $|\phi_m|^2 \geq 1$ , where the former is convex and the latter is not convex. Since the global lower-bound of a convex function  $|\phi_m|^2$  can be expressed by the first-order Taylor expansion at any feasible point, then nonconvex constraint  $|\phi_m|^2 \geq 1$  can be transformed into an affine constraint. Then Problem (40) becomes

$$\max_{\phi, \delta, \mathbf{b}, \mathbf{x}, \mathbf{y}} \sum_{k=0}^K \delta_k - \lambda^{(t)} \sum_{l=1}^{2M} b_l \quad (41a)$$

$$\text{s.t. (28), (33), (35), (38), (24e),} \quad (41b)$$

$$|\phi_m^{(n)}|^2 - 2\text{Re}\{\phi_m^* \phi_m^{(n)}\} \leq b_m - 1, m = 1, \dots, M, \quad (41c)$$

$$|\phi_m|^2 \leq 1 + b_{M+m}, m = 1, \dots, M, \quad (41d)$$

$$\mathbf{b} \succeq \mathbf{0}, \quad (41e)$$

where  $\mathbf{b} = [b_1, \dots, b_{2M}]^T$  are slack variables introduced for the unit-modulus constraints;  $\sum_{l=1}^{2M} b_l$  is added into the objective function as a penalty term; and  $\lambda^{(t)}$  is employed as the regularization factor to control the feasibility of the constraints.

### B. Scenario 2: Full CSI errors

In this section, we extend the OCR-PM problem to the case where both the direct channels  $\mathbf{h}_{ae,k}$  and cascaded channels  $\mathbf{G}_{ce,k}$  from Alice to Eves are imperfect. Considering the full statistical CSI error model in (9), the leakage data rate outage constraints in (11c) for Eve can be extended to

$$\Pr_{\mathbf{g}_{he,k}, \mathbf{g}_{ge,k}} \left\{ \hat{\mathbf{h}}_{e,k}^H [\mathbf{W} - (\beta - 1)\mathbf{Z}] \hat{\mathbf{h}}_{e,k} \leq (\beta - 1)\sigma_{e,k}^2 \right\} \geq 1 - \rho_k, \forall k \in \mathcal{K}. \quad (42)$$

By substituting (8) and (7) into (42), it can be reformulated as

$$\begin{aligned} & \Pr_{\mathbf{g}_{he,k}, \mathbf{g}_{ge,k}} \left\{ [\mathbf{h}_{ae,k}^H + \Delta \mathbf{h}_{ae,k}^H + \boldsymbol{\phi}^T (\bar{\mathbf{G}}_{ce,k} + \Delta \mathbf{G}_{ce,k})] \Xi_e [\mathbf{h}_{ae,k}^H + \Delta \mathbf{h}_{ae,k}^H + \boldsymbol{\phi}^T (\bar{\mathbf{G}}_{ce,k} + \Delta \mathbf{G}_{ce,k})]^H \right. \\ & \quad \left. + \tilde{\sigma}_{e,k}^2 \geq 0 \right\} \\ = & \Pr_{\mathbf{g}_{he,k}, \mathbf{g}_{ge,k}} \left\{ \underbrace{(\Delta \mathbf{h}_{ae,k}^H + \boldsymbol{\phi}^T \Delta \mathbf{G}_{ce,k}) \Xi_e (\Delta \mathbf{h}_{ae,k} + \Delta \mathbf{G}_{ce,k}^H \boldsymbol{\phi}^*)}_{f_{1,k}^{\text{full}}} \right. \\ & \quad \left. + 2\text{Re} \left\{ \underbrace{(\mathbf{h}_{ae,k}^H + \boldsymbol{\phi}^T \bar{\mathbf{G}}_{ce,k}) \Xi_e (\Delta \mathbf{h}_{ae,k} + \Delta \mathbf{G}_{ce,k}^H \boldsymbol{\phi}^*)}_{f_{2,k}^{\text{full}}} \right\} \right. \\ & \quad \left. + \underbrace{(\mathbf{h}_{ae,k}^H + \boldsymbol{\phi}^T \bar{\mathbf{G}}_{ce,k}) \Xi_e (\mathbf{h}_{ae,k}^H + \boldsymbol{\phi}^T \bar{\mathbf{G}}_{ce,k})^H + \tilde{\sigma}_{e,k}^2}_{c_k^{\text{full}}} \geq 0 \right\}. \end{aligned} \quad (43a)$$

In addition to the CSI error vector  $\mathbf{g}_{ge,k}$  for the cascaded channel, we denote the CSI error vector for the direct channel by  $\mathbf{g}_{he,k} \triangleq \Delta \mathbf{h}_{ae,k} = \boldsymbol{\Sigma}_{he,k}^{1/2} \mathbf{v}_{he,k}$ , where  $\mathbf{v}_{he,k} \sim \mathcal{CN}(\mathbf{0}, \mathbf{I}_{N_t})$  and  $\boldsymbol{\Sigma}_{he,k} = \boldsymbol{\Sigma}_{he,k}^{1/2} \boldsymbol{\Sigma}_{he,k}^{1/2}$ . Since  $\boldsymbol{\Sigma}_{he,k}$  is a semidefinite matrix, we have  $(\boldsymbol{\Sigma}_{he,k}^{1/2})^H = \boldsymbol{\Sigma}_{he,k}^{1/2}$  and  $(\boldsymbol{\Sigma}_{he,k}^{1/2})^T = (\boldsymbol{\Sigma}_{he,k}^{1/2})^*$ . By invoking the identity  $\text{Tr}(\mathbf{ABCD}) = \text{vec}^T(\mathbf{D})(\mathbf{A} \otimes \mathbf{C}^T) \text{vec}(\mathbf{B}^T)$ , the expression of

$f_{2,k}^{full}$  can be rewritten as

$$\begin{aligned}
f_{2,k}^{full} &= (\mathbf{h}_{ae,k}^H + \phi^T \bar{\mathbf{G}}_{ce,k}) \Xi_e \Delta \mathbf{h}_{ae,k} + (\mathbf{h}_{ae,k}^H + \phi^T \bar{\mathbf{G}}_{ce,k}) \Xi_e \Delta \mathbf{G}_{ce,k}^H \phi^* \\
&= (\mathbf{h}_{ae,k}^H + \phi^T \bar{\mathbf{G}}_{ce,k}) \Xi_e \mathbf{g}_{he,k} + \text{Tr}[\Xi_e \Delta \mathbf{G}_{ce,k}^H \phi^* (\mathbf{h}_{ae,k}^H + \phi^T \bar{\mathbf{G}}_{ce,k})] \\
&= (\mathbf{h}_{ae,k}^H + \phi^T \bar{\mathbf{G}}_{ce,k}) \Xi_e \mathbf{g}_{he,k} + \text{vec}^T(\mathbf{h}_{ae,k}^H + \phi^T \bar{\mathbf{G}}_{ce,k}) (\Xi_e \otimes \phi^H) \text{vec}(\Delta \mathbf{G}_{ce,k}^*) \\
&= (\mathbf{h}_{ae,k}^H + \phi^T \bar{\mathbf{G}}_{ce,k}) \Xi_e \Sigma_{he,k}^{1/2} \mathbf{v}_{he,k} + (\mathbf{h}_{ae,k}^H + \phi^T \bar{\mathbf{G}}_{ce,k}) (\Xi_e \otimes \phi^H) \Sigma_{ge,k}^{1/2*} \mathbf{v}_{ge,k}^* \\
&= \tilde{\mathbf{u}}_{e,k}^H \tilde{\mathbf{v}}_{e,k},
\end{aligned} \tag{44}$$

where  $\tilde{\mathbf{v}}_{e,k} = [\mathbf{v}_{he,k}^H, \mathbf{v}_{ge,k}^T]^H$ , and

$$\begin{aligned}
\tilde{\mathbf{u}}_{e,k} &= \begin{bmatrix} \Sigma_{he,k}^{1/2} \Xi_e (\mathbf{h}_{ae,k} + \bar{\mathbf{G}}_{ce,k}^H \phi^*) \\ \Sigma_{ge,k}^{1/2T} (\Xi_e \otimes \phi) (\mathbf{h}_{ae,k} + \bar{\mathbf{G}}_{ce,k}^H \phi^*) \end{bmatrix} \stackrel{(k)}{=} \begin{bmatrix} \Sigma_{he,k}^{1/2} \Xi_e (\mathbf{h}_{ae,k} + \bar{\mathbf{G}}_{ce,k}^H \phi^*) \\ \Sigma_{ge,k}^{1/2T} ([\Xi_e (\mathbf{h}_{ae,k} + \bar{\mathbf{G}}_{ce,k}^H \phi^*)] \otimes \phi) \end{bmatrix} \\
&= \begin{bmatrix} \Sigma_{he,k}^{1/2} \Xi_e (\mathbf{h}_{ae,k} + \bar{\mathbf{G}}_{ce,k}^H \phi^*) \\ \Sigma_{ge,k}^{1/2T} ([\Xi_e (\mathbf{h}_{ae,k} + \bar{\mathbf{G}}_{ce,k}^H \phi^*)] \otimes (\mathbf{I}_M \phi)) \end{bmatrix} \\
&= \begin{bmatrix} \Sigma_{he,k}^{1/2} \Xi_e (\mathbf{h}_{ae,k} + \bar{\mathbf{G}}_{ce,k}^H \phi^*) \\ \Sigma_{ge,k}^{1/2T} (\Xi_e \otimes \mathbf{I}_M) ((\mathbf{h}_{ae,k} + \bar{\mathbf{G}}_{ce,k}^H \phi^*) \otimes \phi) \end{bmatrix}.
\end{aligned} \tag{45}$$

The the step in (k) in (45) is obtained by invoking the property  $(\mathbf{A} \otimes \mathbf{b})\mathbf{c} = (\mathbf{A}\mathbf{c}) \otimes \mathbf{b}$ , when  $\mathbf{b}$  and  $\mathbf{c}$  are column vectors. The expression of  $f_{1,k}^{full}$  can be rewritten as

$$\begin{aligned}
f_{1,k}^{full} &= \Delta \mathbf{h}_{ae,k}^H \Xi_e \Delta \mathbf{h}_{ae,k} + \phi^T \Delta \mathbf{G}_{ce,k} \Xi_e \Delta \mathbf{G}_{ce,k}^H \phi^* + 2\text{Re}\{\Delta \mathbf{h}_{ae,k}^H \Xi_e \Delta \mathbf{G}_{ce,k}^H \phi^*\} \\
&= \Delta \mathbf{h}_{ae,k}^H \Xi_e \Delta \mathbf{h}_{ae,k} + \text{Tr}(\Xi_e \Delta \mathbf{G}_{ce,k}^H \mathbf{E} \Delta \mathbf{G}_{ce,k}) + 2\text{Re}\{\text{Tr}(\Xi_e \Delta \mathbf{G}_{ce,k}^H \phi^* \Delta \mathbf{h}_{ae,k}^H)\} \\
&\stackrel{(l)}{=} \Delta \mathbf{h}_{ae,k}^H \Xi_e \Delta \mathbf{h}_{ae,k} + \text{vec}^T(\Delta \mathbf{G}_{ce,k}) (\Xi_e \otimes \mathbf{E}^T) \text{vec}(\Delta \mathbf{G}_{ce,k}^*) \\
&\quad + 2\text{Re}\{\text{vec}^T(\Delta \mathbf{h}_{ae,k}^H) (\Xi_e \otimes \phi^H) \text{vec}(\Delta \mathbf{G}_{ce,k}^*)\} \\
&= \mathbf{v}_{he,k}^H \Sigma_{he,k}^{1/2} \Xi_e \Sigma_{he,k}^{1/2} \mathbf{v}_{he,k} + \mathbf{v}_{ge,k}^T \Sigma_{ge,k}^{1/2T} (\Xi_e \otimes \mathbf{E}^T) \Sigma_{ge,k}^{1/2*} \mathbf{v}_{ge,k}^* \\
&\quad + 2\text{Re}\{\mathbf{v}_{he,k}^H \Sigma_{he,k}^{1/2} (\Xi_e \otimes \phi^H) \Sigma_{ge,k}^{1/2*} \mathbf{v}_{ge,k}^*\} \\
&= \tilde{\mathbf{v}}_{e,k}^H \tilde{\mathbf{A}}_{e,k} \tilde{\mathbf{v}}_{e,k},
\end{aligned} \tag{46}$$

where (l) is obtained by invoking  $\text{Tr}(\mathbf{ABCD}) = \text{vec}^T(\mathbf{D})(\mathbf{A} \otimes \mathbf{C}^T) \text{vec}(\mathbf{B}^T)$ , and

$$\tilde{\mathbf{A}}_{e,k} = \begin{bmatrix} \Sigma_{he,k}^{1/2} \Xi_e \Sigma_{he,k}^{1/2} & \Sigma_{he,k}^{1/2} (\Xi_e \otimes \phi^H) \Sigma_{ge,k}^{1/2*} \\ \Sigma_{ge,k}^{1/2T} (\Xi_e \otimes \phi) \Sigma_{he,k}^{1/2} & \Sigma_{ge,k}^{1/2T} (\Xi_e \otimes \mathbf{E}^T) \Sigma_{ge,k}^{1/2*} \end{bmatrix}. \tag{47}$$

Then, the outage constraint (43b) is recast as

$$\Pr_{\mathbf{g}_{h,e,k}, \mathbf{g}_{g,e,k}} \left\{ \tilde{\mathbf{v}}_{e,k}^H \tilde{\mathbf{A}}_{e,k} \tilde{\mathbf{v}}_{e,k} + 2\text{Re}\{\tilde{\mathbf{u}}_{e,k}^H \tilde{\mathbf{v}}_{e,k}\} + c_k^{\text{full}} \geq 0 \right\} \geq 1 - \rho_k, \forall k \in \mathcal{K}, \quad (48)$$

By invoking Lemma 1 and introducing the slack variables  $\tilde{\mathbf{x}} = [\tilde{x}_1, \tilde{x}_2, \dots, \tilde{x}_K]^T$  and  $\tilde{\mathbf{y}} = [\tilde{y}_1, \tilde{y}_2, \dots, \tilde{y}_K]^T$ , we arrive at the desired safe approximation of OCR-PM under the full channel uncertainty, which is shown as

$$\min_{\mathbf{W}, \mathbf{Z}, \phi, \tilde{\mathbf{A}}, \tilde{\mathbf{x}}, \tilde{\mathbf{y}}} \text{Tr}(\mathbf{W} + \mathbf{Z}) \quad (49a)$$

$$\text{s.t.} \quad \text{Tr}(\tilde{\mathbf{A}}_{e,k}) - \sqrt{-2 \ln(\rho_k)} \cdot \tilde{x}_k + \ln(\rho_k) \cdot \tilde{y}_k + c_k^{\text{full}} \geq 0, \quad (49b)$$

$$\left\| \begin{bmatrix} \text{vec}(\tilde{\mathbf{A}}_{e,k}) \\ \sqrt{2} \tilde{\mathbf{u}}_{e,k} \end{bmatrix} \right\|_2 \leq \tilde{x}_k, \quad (49c)$$

$$\tilde{y}_k \mathbf{I}_{MN_t} + \tilde{\mathbf{A}}_k \succeq \mathbf{0}, \tilde{y}_k \geq 0, \quad (49d)$$

$$(11b), (10d), (10e), (10f), (10g), \quad (49e)$$

where  $\tilde{\mathbf{A}}_e = [\tilde{\mathbf{A}}_{e,1}, \tilde{\mathbf{A}}_{e,2}, \dots, \tilde{\mathbf{A}}_{e,K}]$ . We utilize the AO method to decouple the variables. When  $\phi$  is fixed, the  $\tilde{\mathbf{A}}_{e,k}$  and  $\tilde{\mathbf{u}}_{e,k}$  are linear function of the  $\mathbf{W}$  and  $\mathbf{Z}$ . Then, the  $\mathbf{W}$  and  $\mathbf{Z}$  can be obtained by the SDR technique, and the  $\{\mathbf{W}^{(n)}, \mathbf{Z}^{(n)}\}$  obtained at the  $n$ th iteration are given as

$$\{\mathbf{W}^{(n)}, \mathbf{Z}^{(n)}\} = \arg \min_{\mathbf{W}, \mathbf{Z}, \mathbf{x}, \mathbf{y}} \text{Tr}(\mathbf{W} + \mathbf{Z}) \quad (50a)$$

$$\text{s.t.} \quad (49b), (49c), (49d), (11b), (10d), (10e). \quad (50b)$$

When  $\mathbf{W}$  and  $\mathbf{Z}$  are fixed, the optimization problem for  $\phi$  becomes a feasibility check problem. Similarly, the slack variables  $\boldsymbol{\delta} = [\delta_0, \delta_1, \delta_2, \dots, \delta_K]^T$  are introduced to improve the convergence of the AO algorithm. The constraints in Problem (49) must be transformed into convex constraints. We have the following steps:

**Step 1:** Transform the constraint in (49b) to be convex.

We find that  $c_k^{\text{full}} = c_k^{\text{partial}}$ , thus the process on  $c_k^{\text{full}}$  is the same as the process on  $c_k^{\text{partial}}$  under the partial channel uncertainty. Then we have  $c_k^{\text{full}} = (25)$ , the expression of which is concave w.r.t.  $\phi$ . The  $\text{Tr}[\tilde{\mathbf{A}}_{e,k}]$  are transformed as

$$\begin{aligned} \text{Tr}[\tilde{\mathbf{A}}_{e,k}] &= \text{Tr}[\boldsymbol{\Sigma}_{he,k}^{1/2} \boldsymbol{\Xi}_e \boldsymbol{\Sigma}_{he,k}^{1/2}] + \left\{ \text{Tr}[\boldsymbol{\Sigma}_{ge,k}^{1/2T} (\boldsymbol{\Xi}_e \otimes \mathbf{E}^T) \boldsymbol{\Sigma}_{ge,k}^{1/2*}] \right\}^* \\ &\stackrel{(m)}{=} \text{Tr}[\boldsymbol{\Sigma}_{he,k}^{1/2} \boldsymbol{\Xi}_e \boldsymbol{\Sigma}_{he,k}^{1/2}] + \text{Tr}[\boldsymbol{\Sigma}_{ge,k}^{1/2H} (\boldsymbol{\Xi}_e^T \otimes \mathbf{E}) \boldsymbol{\Sigma}_{ge,k}^{1/2}] \\ &\stackrel{(n)}{=} \text{Tr}[\boldsymbol{\Sigma}_{he,k}^{1/2} \boldsymbol{\Xi}_e \boldsymbol{\Sigma}_{he,k}^{1/2}] + \phi^T \boldsymbol{\Sigma}_{gx,k} (\mathbf{I}_{MN_t} \otimes \boldsymbol{\Xi}_e) \boldsymbol{\Sigma}_{gx,k}^H \phi^*, \end{aligned} \quad (51)$$

where the second term of (m) is the same as the  $\text{Tr}[\mathbf{A}_{e,k}]$  under the partial channel uncertainty, and the second term of (n) is obtained in the same way of (26). The second term in (n) of (51) is equivalently transformed to be concave w.r.t.  $\phi$  as in (27). By substituting (27) into (51), we reformulate (51) to a concave form as

$$\text{Tr}[\tilde{\mathbf{A}}_{e,k}] = \text{Tr}[\Sigma_{he,k}^{1/2} \Xi_e \Sigma_{he,k}^{1/2}] + \phi^T [\Sigma_{gx,k} (\mathbf{I}_{MN_t} \otimes \Xi_e) \Sigma_{gx,k}^H - c_{t,k} \mathbf{I}_M] \phi^* + M c_{t,k}. \quad (52)$$

By substituting (25) and (52) into the constraint in (49b), we can obtain a convex constraint equivalent to (49b) as

$$(49b) \Leftrightarrow c_{tc,k}^{\text{full}}(\phi) \geq 0, \quad (53)$$

which is convex, and

$$\begin{aligned} c_{tc,k}^{\text{full}}(\phi) &\triangleq \text{Tr}[\Sigma_{he,k}^{1/2} \Xi_e \Sigma_{he,k}^{1/2}] + \phi^T [\Sigma_{gx,k} (\mathbf{I}_{MN_t} \otimes \Xi_e) \Sigma_{gx,k}^H - c_{t,k} \mathbf{I}_M] \phi^* + M c_{t,k} \\ &\quad - \sqrt{-2 \ln(\rho_k)} \cdot x_k + \ln(\rho_k) \cdot y_k + \phi^T (\bar{\mathbf{G}}_{ce,k} \Xi_e \bar{\mathbf{G}}_{ce,k}^H - c_{c,k} \mathbf{I}_M) \phi^* \\ &\quad + 2 \text{Re}\{\phi^T \bar{\mathbf{G}}_{ce,k} \Xi_e \mathbf{h}_{ae,k}\} + \mathbf{h}_{ae,k}^H \Xi_e \mathbf{h}_{ae,k} + M c_{c,k} + \tilde{\sigma}_{e,k}^2 + \delta_k. \end{aligned} \quad (54)$$

**Step2:** Transform the constraint in (49c) to be convex.

We can find an upper bound of the left hand side of constraint (49c) as follows:

$$\begin{aligned} \left\| \text{vec}(\tilde{\mathbf{A}}_{e,k}) \right\|^2 &= \left\| \Sigma_{he,k}^{1/2} \Xi_e \Sigma_{he,k}^{1/2} \right\|^2 + 2 \left\| \Sigma_{ge,k}^{1/2T} (\Xi_e \otimes \phi) \Sigma_{he,k}^{1/2} \right\|^2 + \left\| \Sigma_{ge,k}^{1/2T} (\Xi_e \otimes \mathbf{E}^T) \Sigma_{ge,k}^{1/2*} \right\|^2 \\ &\stackrel{(o)}{=} \left\| (\Sigma_{he,k}^{1/2T} \otimes \Sigma_{he,k}^{1/2}) \text{vec}(\Xi_e) \right\|^2 + 2 \left\| (\Sigma_{he,k}^{1/2T} \otimes \Sigma_{ge,k}^{1/2*}) \text{vec}(\Xi_e \otimes \phi) \right\|^2 \\ &\quad + \left\| (\Sigma_{ge,k}^{1/2} \otimes \Sigma_{ge,k}^{1/2*}) \text{vec}(\Xi_e \otimes \mathbf{E}^T) \right\|^2 \end{aligned} \quad (55)$$

$$\begin{aligned} &\Rightarrow \stackrel{(p)}{\leq} \sigma_{\max}^2(\Sigma_{he,k}^{1/2T} \otimes \Sigma_{he,k}^{1/2}) \|\Xi_e\|_F^2 + 2 \sigma_{\max}^2(\Sigma_{he,k}^{1/2T} \otimes \Sigma_{ge,k}^{1/2*}) M \|\Xi_e\|_F^2 \\ &\quad + \sigma_{\max}^2(\Sigma_{ge,k}^{1/2} \otimes \Sigma_{ge,k}^{1/2*}) M^2 \|\Xi_e\|_F^2 \\ &\Rightarrow \stackrel{(q)}{\leq} \left| \lambda_{\max}(\Sigma_{he,k}^T) + \lambda_{\max}(\Sigma_{ge,k}^*) M \right|^2 \|\Xi_e\|_F^2 \end{aligned} \quad (56)$$

$$\Rightarrow \left\| \text{vec}(\tilde{\mathbf{A}}_{e,k}) \right\| \leq \left| \lambda_{\max}(\Sigma_{he,k}^T) + \lambda_{\max}(\Sigma_{ge,k}^*) M \right| \|\Xi_e\|_F. \quad (57)$$

$$\begin{aligned}
\|\tilde{\mathbf{u}}_{e,k}\|^2 &= \left\| \begin{array}{c} \boldsymbol{\Sigma}_{he,k}^{1/2} \boldsymbol{\Xi}_e (\mathbf{h}_{ae,k} + \bar{\mathbf{G}}_{ce,k}^H \boldsymbol{\phi}^*) \\ \boldsymbol{\Sigma}_{ge,k}^{1/2T} (\boldsymbol{\Xi}_e \otimes \mathbf{I}_M) ((\mathbf{h}_{ae,k} + \bar{\mathbf{G}}_{ce,k}^H \boldsymbol{\phi}^*) \otimes \boldsymbol{\phi}) \end{array} \right\|^2 \\
&= \left\| \boldsymbol{\Sigma}_{he,k}^{1/2} \boldsymbol{\Xi}_e (\mathbf{h}_{ae,k} + \bar{\mathbf{G}}_{ce,k}^H \boldsymbol{\phi}^*) \right\|^2 + \left\| \boldsymbol{\Sigma}_{ge,k}^{1/2T} (\boldsymbol{\Xi}_e \otimes \mathbf{I}_M) ((\mathbf{h}_{ae,k} + \bar{\mathbf{G}}_{ce,k}^H \boldsymbol{\phi}^*) \otimes \boldsymbol{\phi}) \right\|^2 \\
&\stackrel{(r)}{\leq} \sigma_{\max}^2(\boldsymbol{\Sigma}_{he,k}^{1/2} \boldsymbol{\Xi}_e) \|\mathbf{h}_{ae,k} + \bar{\mathbf{G}}_{ce,k}^H \boldsymbol{\phi}^*\|^2 + \sigma_{\max}^2(\boldsymbol{\Sigma}_{ge,k}^{1/2T} (\boldsymbol{\Xi}_e \otimes \mathbf{I}_M)) M^2 \|\mathbf{h}_{ae,k} + \bar{\mathbf{G}}_{ce,k}^H \boldsymbol{\phi}^*\|^2 \\
&\leq [\lambda_{\max}^2(\boldsymbol{\Sigma}_{he,k}^{1/2} \boldsymbol{\Xi}_e) + \lambda_{\max}^2(\boldsymbol{\Sigma}_{ge,k}^{1/2T} (\boldsymbol{\Xi}_e \otimes \mathbf{I}_M)) M^2] \|\mathbf{h}_{ae,k} + \bar{\mathbf{G}}_{ce,k}^H \boldsymbol{\phi}^*\|^2, \tag{58}
\end{aligned}$$

where the proof for (o) is given in Appendix B. The (p) is obtained by using  $\|\mathbf{Ax}\|_2 \leq \|\mathbf{A}\|_2 \|\mathbf{x}\|_2$ ,  $\|\mathbf{A}\|_2 = \sigma_{\max}\{\mathbf{A}\}$  and the property in (31). The (q) is obtained due to  $\text{eig}(\mathbf{A} \otimes \mathbf{B}) = \text{eig}(\mathbf{A}) \otimes \text{eig}(\mathbf{B})$  and  $\sigma_{\max}\{\mathbf{A}\} = \lambda_{\max}\{\mathbf{A}\}$  when  $\mathbf{A} \in \mathbb{H}^n$ . The (r) is obtained due to  $\|\mathbf{b} \otimes \mathbf{c}\| = \|\mathbf{b}\| \|\mathbf{c}\|$ . By utilizing the upper bounds in (57) and (58), we consider the following constraint instead of the original constraint (49c) as

$$\left\| \frac{\lambda_{\max}(\boldsymbol{\Sigma}_{he,k}^{1/2T}) + \lambda_{\max}(\boldsymbol{\Sigma}_{ge,k}^{1/2*}) M \text{vec}(\boldsymbol{\Xi}_e)}{\sqrt{2[\lambda_{\max}^2(\boldsymbol{\Sigma}_{he,k}^{1/2} \boldsymbol{\Xi}_e) + \lambda_{\max}^2(\boldsymbol{\Sigma}_{ge,k}^{1/2T} (\boldsymbol{\Xi}_e \otimes \mathbf{I}_M)) M^2]} (\mathbf{h}_{ae,k} + \bar{\mathbf{G}}_{ce,k}^H \boldsymbol{\phi})} \right\| \leq \tilde{x}_k. \tag{59}$$

It is readily to check that when (59) holds, the original constraint (49c) always holds.

**Step3:** Transform the constraint in (49d) to be convex.

The transformation is similar as the process in (34d). By moving  $\tilde{\mathbf{A}}_k$  in (49d) from the left hand side to the right hand side of the inequality sign, we have

$$\tilde{y}_k \mathbf{I}_{MN_t} \succeq -\tilde{\mathbf{A}}_k. \tag{60}$$

Then, we define a matrix as

$$\mathbf{B}_{e,k} = \begin{bmatrix} \boldsymbol{\Sigma}_{he,k}^{1/2} (c_g \mathbf{I}_{N_t}) \boldsymbol{\Sigma}_{he,k}^{1/2} & \boldsymbol{\Sigma}_{he,k}^{1/2} (c_g \mathbf{I}_{N_t} \otimes \boldsymbol{\phi}^H) \boldsymbol{\Sigma}_{ge,k}^{1/2*} \\ \boldsymbol{\Sigma}_{ge,k}^{1/2T} (c_g \mathbf{I}_{N_t} \otimes \boldsymbol{\phi}) \boldsymbol{\Sigma}_{he,k}^{1/2} & \boldsymbol{\Sigma}_{ge,k}^{1/2T} (c_g \mathbf{I}_{N_t} \otimes \mathbf{E}^T) \boldsymbol{\Sigma}_{ge,k}^{1/2*} \end{bmatrix}. \tag{61}$$

By adding the matrix  $\mathbf{B}_{e,k}$  on both sides of the inequality in (60), we have

$$\begin{aligned}
y_k \mathbf{I}_{(N_t M + N_t)} + \mathbf{B}_{e,k} &\succeq \begin{bmatrix} \Sigma_{he,k}^{1/2} (c_g \mathbf{I}_{N_t}) \Sigma_{he,k}^{1/2} & \Sigma_{he,k}^{1/2} (c_g \mathbf{I}_{N_t} \otimes \phi^H) \Sigma_{ge,k}^{1/2*} \\ \Sigma_{ge,k}^{1/2T} (c_g \mathbf{I}_{N_t} \otimes \phi) \Sigma_{he,k}^{1/2} & \Sigma_{ge,k}^{1/2T} (c_g \mathbf{I}_{N_t} \otimes \mathbf{E}^T) \Sigma_{ge,k}^{1/2*} \end{bmatrix} \\
&\quad - \begin{bmatrix} \Sigma_{he,k}^{1/2} \Xi_e \Sigma_{he,k}^{1/2} & \Sigma_{he,k}^{1/2} (\Xi_e \otimes \phi^H) \Sigma_{ge,k}^{1/2*} \\ \Sigma_{ge,k}^{1/2T} (\Xi_e \otimes \phi) \Sigma_{he,k}^{1/2} & \Sigma_{ge,k}^{1/2T} (\Xi_e \otimes \mathbf{E}^T) \Sigma_{ge,k}^{1/2*} \end{bmatrix} \\
\Leftrightarrow y_k \mathbf{I}_{(N_t M + N_t)} + \mathbf{B}_{e,k} &\succeq \begin{bmatrix} \Sigma_{he,k}^{1/2} (\mathbf{V}_{wgz} \mathbf{V}_{wgz}^H) \Sigma_{he,k}^{1/2} & \Sigma_{he,k}^{1/2} ((\mathbf{V}_{wgz} \mathbf{V}_{wgz}^H) \otimes \phi^H) \Sigma_{ge,k}^{1/2*} \\ \Sigma_{ge,k}^{1/2T} ((\mathbf{V}_{wgz} \mathbf{V}_{wgz}^H) \otimes \phi) \Sigma_{he,k}^{1/2} & \Sigma_{ge,k}^{1/2T} ((\mathbf{V}_{wgz} \mathbf{V}_{wgz}^H) \otimes \mathbf{E}^T) \Sigma_{ge,k}^{1/2*} \end{bmatrix} \\
\Leftrightarrow y_k \mathbf{I}_{(N_t M + N_t)} + \mathbf{B}_{e,k} &\succeq \begin{bmatrix} \Sigma_{he,k}^{1/2} \mathbf{V}_{wgz} \\ \Sigma_{ge,k}^{1/2T} (\mathbf{V}_{wgz} \otimes \phi) \end{bmatrix} \begin{bmatrix} \mathbf{V}_{wgz}^H \Sigma_{he,k}^{1/2} & (\mathbf{V}_{wgz}^H \otimes \phi^H) \Sigma_{ge,k}^{1/2*} \end{bmatrix}. \quad (62)
\end{aligned}$$

Similarly, we find that  $\lambda_{\min}\{\mathbf{B}_{e,k}\} = 0$ , which is proved in Appendix D. Thus, we have the convex LMI inequality constraint as

$$\begin{aligned}
(49d) \Leftrightarrow \tilde{y}_k &\stackrel{(s)}{\geq} \left\| \begin{bmatrix} \Sigma_{he,k}^{1/2} \mathbf{V}_{wgz} \\ \Sigma_{ge,k}^{1/2T} (\mathbf{V}_{wgz} \otimes \phi) \end{bmatrix} \right\|_2, \tilde{y}_k \geq 0, \\
&\Leftrightarrow \left\| \begin{bmatrix} \Sigma_{he,k}^{1/2} \mathbf{V}_{wgz} \\ \Sigma_{ge,k}^{1/2T} (\mathbf{V}_{wgz} \otimes \phi) \end{bmatrix} \right\|_2 - \tilde{y}_k \leq 0, \tilde{y}_k \geq 0, \quad (63)
\end{aligned}$$

where (s) is obtained due to  $\|\mathbf{A}\|_2 = \sqrt{\max \text{eig}(\mathbf{A}^H \mathbf{A})}$ .

Finally, based on the mathematical manipulations of Steps 1-3 above and by using the CCP method, the problem for optimizing  $\phi$  can be reformulated as

$$\max_{\phi, \delta, \mathbf{x}, \mathbf{y}} \sum_{k=0}^K \delta_k - \lambda^{(t)} \sum_{l=1}^{2M} b_l \quad (64a)$$

$$\text{s.t. (53), (59), (63), (38), (24e),} \quad (64b)$$

$$(41c), (41d), (41e). \quad (64c)$$

The same techniques under the partial channel uncertainty can be utilized here to solve Problem (64), which is omitted to make the paper compact.

## IV. SIMULATION RESULTS

### A. Simulation Setup

The simulation setup is shown in Fig. 2. The Alice is located at (5,0,20) m, the IRS is located at (0,50,2) m, the Bob is located at (3,50,0) m. The Eves are randomly distributed on the line from (2,45,0) m to (2,55,0) m.

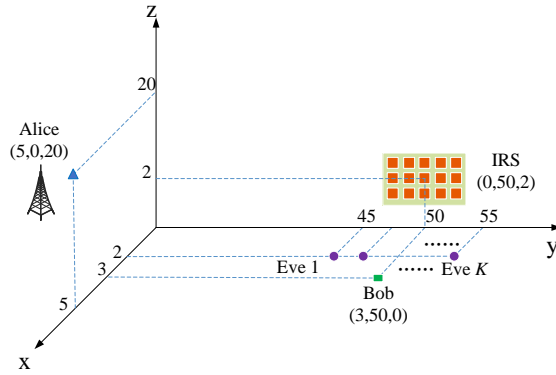


Fig. 2. The simulated secure communication scenario

The channel matrix between Alice and the IRS is modeled as  $\mathbf{G}_{ar} \in \mathbb{C}^{M \times N_t}$ , which is

$$\mathbf{G}_{ar}^T = \sqrt{L_0 d_{ar}^{-\alpha_{ar}}} \left( \sqrt{\frac{\beta_{ar}}{1 + \beta_{ar}}} \mathbf{G}_{ar}^{LOS} + \sqrt{\frac{1}{1 + \beta_{ar}}} \mathbf{G}_{ar}^{NLOS} \right), \quad (65)$$

where  $L_0$  denote the pathloss at the distance of 1m, and is set to be  $-40$  dB based on the 3GPP UMi model [32] with 3.5 GHz carrier frequency (i.e., carrier frequency of 5G in China). The distance between Alice and the IRS is denoted by  $d_{ar}$ , while  $\alpha_{ar}$  denotes the corresponding path loss exponent. The small-scale fading is assumed to be Rician fading with Rician factor  $\beta_{ar}$ . The  $\mathbf{G}_{ar}^{LOS}$  and  $\mathbf{G}_{ar}^{NLOS}$  denotes the line of sight (LoS) component and the non-LoS (NLoS) component of the Alice-IRS channel respectively. The  $\mathbf{G}_{ar}^{LOS}$  can be modeled as  $\mathbf{G}_{ar}^{LOS} = \mathbf{c}\mathbf{d}^H$ , where  $\mathbf{c} = [c_1, c_2, \dots, c_{N_t}]^T$  denotes the transmit steering vector of Alice, and  $\mathbf{d} = [d_1, d_2, \dots, d_M]^T$  denotes the receive steering vector of the IRS.  $\mathbf{G}_{ar}^{NLOS}$  is modeled as Rayleigh fading. The channels of the IRS-Bob link, IRS-Eve link, Alice-Bob link, and Alice-Eve link are modeled similarly.

The other parameters are as follows. The path loss exponent for Alice-IRS channel is set as  $\alpha_{ar} = 2.2$ . The IRS-Bob channels  $\alpha_{rb}$  and IRS-Eve channels  $\alpha_{re}$  are set as  $\alpha_{rb} = \alpha_{re} = 2$ . A more scattering environment is assumed for the direct links, thus the path loss exponents for Alice-Bob channel and Alice-Eve channel are set as  $\alpha_{ab} = \alpha_{ae} = 3.5$ . The Rician factors for the Alice-IRS channel  $\beta_{ar}$ , IRS-Bob channel  $\beta_{rb}$ , IRS-Eve channel  $\beta_{re}$ , Alice-Bob channel  $\beta_{ab}$ , Alice-Eve channel  $\beta_{ae}$  are set to be the same and equal to 5. The noise power at Bob and Eves is set as  $\sigma_b^2 = \sigma_{e,k}^2 = -85$  dBm. The convergence tolerance is  $\varepsilon = 10^{-3}$ . The outage probability is  $\rho_k = 0.05$ . For the statistical cascaded CSI error model, the variance matrix of  $\mathbf{g}_{ge,k}$  is defined as  $\Sigma_{ge,k} = \varepsilon_{g,k}^2 \mathbf{I}$ , where  $\varepsilon_{g,k}^2 = \delta_{g,k}^2 \|\text{vec}(\bar{\mathbf{G}}_{ce,k})\|_2^2$ , while the variance matrix of  $\mathbf{g}_{he,k}$  is defined as

$\Sigma_{he,k} = \varepsilon_{h,k}^2 \mathbf{I}$ , where  $\varepsilon_{h,k}^2 = \delta_{h,k}^2 \|\bar{\mathbf{h}}_{ae,k}\|_2^2$ .  $\delta_{g,k}, \delta_{h,k} \in [0, 1)$  are the normalized CSI errors, which measure the relative amount of CSI uncertainties.

### B. Benchmark Schemes

The proposed AO algorithm is compared with the following benchmark schemes:

- **Random-MRT:** It performs maximum ratio transmission (MRT) based beamforming design, i.e.,  $\mathbf{w} = \sqrt{p_w} \frac{\hat{\mathbf{h}}_b}{\|\hat{\mathbf{h}}_b\|} = \sqrt{p_w} \frac{\mathbf{G}_{ar}^H \Phi^H \mathbf{h}_{rb}}{\|\hat{\mathbf{h}}_b\|}$ , where  $p_w$  is the power allocated to Bob. It applies an isotropic AN [33], i.e., the AN covariance matrix is chosen as  $\mathbf{Z} = p_z \mathbf{P}_{\hat{\mathbf{h}}_b}^\perp$ , where  $\mathbf{P}_{\hat{\mathbf{h}}_b}^\perp = \mathbf{I}_{N_t} - \hat{\mathbf{h}}_b \hat{\mathbf{h}}_b^H / \|\hat{\mathbf{h}}_b\|^2$  is the orthogonal complement projector of  $\hat{\mathbf{h}}_b$ , and  $p_z$  is the power invested on AN. For Random-MRT schemes, we assume that the phase shifts  $\Phi$  in  $\hat{\mathbf{h}}_b = \mathbf{h}_{ab} + \mathbf{G}_{ar}^H \Phi^H \mathbf{h}_{rb}$  and  $\hat{\mathbf{h}}_{e,k} = \mathbf{h}_{ae,k} + \mathbf{G}_{ar}^H \Phi^H \mathbf{h}_{re,k}$  are randomly chosen. The allocated power  $p_w$  and  $p_z$  is optimized to satisfy the secrecy constraints in Problem (22) and Problem (50).
- **Optimized-MRT:** Based on the MRT beamforming and isotropic AN, the phase shifts  $\Phi$  of IRS is optimized by the proposed method. The allocated power  $p_w$  and  $p_z$  are optimized to satisfy the secrecy constraints in Problem (22) and Problem (50).
- **Random-IRS:** The phase shifts of IRS  $\Phi$  is randomly selected. The beamforming matrix  $\mathbf{W}$  and AN covariance matrix  $\mathbf{Z}$  are optimized by solving Problem (22) and Problem (50).

### C. Convergence Performance

The convergence performance of the proposed method is investigated in Fig. 3, where two scenarios of partial channel uncertainty and full channel uncertainty for the eavesdroppers are considered. It is observed that the proposed algorithm monotonically converges with different values of  $N_t$ ,  $M$ , and  $K$  for both the partial and Full Eves' CSI errors. The convergence speed decreases with the increased number of IRS reflecting elements  $M$  and the number of eavesdroppers  $K$ , while the convergence speed increases with the increased number of the transmit antennas  $N_t$ . In addition, the number of iterations required for convergence is more sensitive to  $M$  than  $N_t$  and  $K$ . When  $M$  increases from 8 to 17, the required iterations increase from 48 to 64 for partial CSI errors and from 28 to 70 for full CSI errors. As observed in Fig. 3, the convergence speed with partial CSI error is generally slower than that of full CSI error, except the case when the  $M$  is relatively large. Since the dimensions of the search space in the optimization subproblems increase with  $N_t$  and  $M$ , and that the number of constraints in the optimization subproblems increases with  $K$ , the running time of the proposed algorithm always increases with  $N_t$ ,  $K$  and  $M$ .

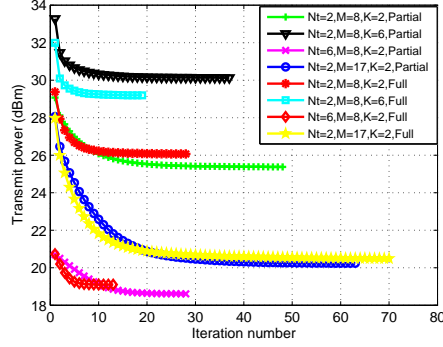


Fig. 3. Convergence of the proposed algorithm. For partial Eves' CSI error, the normalized CSI error is  $\delta_{g,k} = 0.01, \forall k$ , and for full Eves' CSI error, the normalized CSI error is  $\delta_{g,k} = \delta_{h,k} = 0.01, \forall k$ .

#### D. Transmit Power Versus the Minimum Channel Capacity of the Legitimate User

In Fig. 4, we show the transmit power versus the minimum channel capacity  $\log \gamma$  of the legitimate user, while limiting the information leakage to the potential eavesdroppers as  $\log \beta = 0.5$  bit/s/Hz. It is observed from Fig. 4 that the transmit power increases monotonically with the minimum channel capacity of Bob. This is because more transmit power is required to satisfy the increased data rate requirement of Bob. Compared with the other three benchmark schemes, the transmit power budget of the proposed algorithm is the lowest, which demonstrates the superiority of the proposed algorithm. When  $\log \gamma$  is relatively small, the transmit power of the Optimized-MRT scheme is close to that of the proposed algorithm, and lower than that of the Random-IRS scheme. For the Optimized-MRT scheme, the AN is isotropically distributed on the orthogonal complement subspace of the equivalent channel of legitimate user, which is low but enough to limit the data rate of the Eves in addition to confusing the Eves by Eves' CSI error. Moreover, since the AN does not interfere with the legitimate user, and the phase shifts of the IRS are optimized, the relatively small data rate requirement of Bob can be satisfied. However, when  $\log \gamma$  is large, more transmit power is required for Bob, and at the same time, more AN power is required to interfere Eves. Thus, the advantage of the proposed algorithm with more sophisticated design on the beamforming and the AN becomes prominent. By comparing the transmit power of the two scenarios of partial and full CSI errors, we find that when  $\log \gamma$  is small, the transmit power of all these schemes with full CSI errors is smaller than that with partial CSI errors. When  $\log \gamma$  is large, the transmit power with full CSI errors is slightly larger than that with partial CSI errors. This is because when  $\log \gamma$  is small, the full CSI errors for Eves are larger than the partial CSI

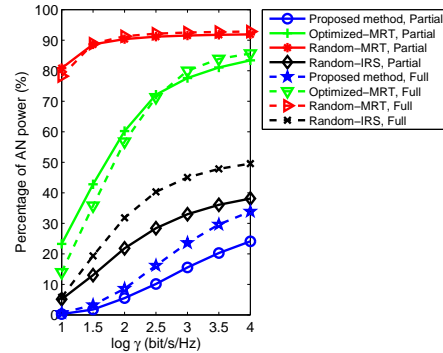
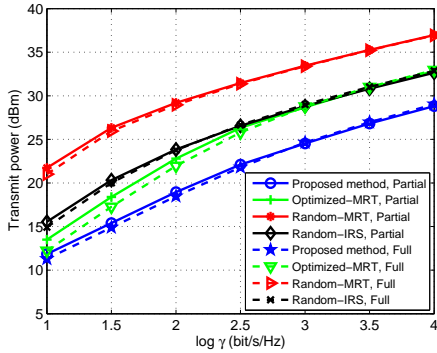


Fig. 4. Transmit power versus the minimum channel capacity  $\log \gamma$  of the legitimate user with  $N_t = 2$ ,  $M = 15$ ,  $K = 2$  and  $\log \beta = 0.5$  bit/s/Hz. For partial Eves' CSI error, the normalized CSI error is  $\delta_{g,k} = 0.01, \forall k$ , and for full Eves' CSI error, the normalized CSI error is  $\delta_{g,k} = \delta_{h,k} = 0.01, \forall k$ .

errors for Eves, thus are good for impairing the Eves. When  $\log \gamma$  is large, more transmit power is required, thus neither the full CSI errors or the partial CSI errors are enough for impairing the Eves, and more AN power is required for interfering the Eves. Then the robust design with full CSI errors require more transmit power to interfere the Eves more effectively.

The percentage of AN power in the total transmit power versus the minimum channel capacity  $\log \gamma$  of the legitimate user is shown in Fig. 5. It is seen from Fig. 5 that the percentage of the AN power for the MRT strategy is much higher than that for the Random-IRS scheme and the proposed scheme. That's because the AN in the MRT strategy is isotropically distributed, while the AN in the Random-IRS scheme and the proposed algorithm is spatially focused. With increased  $\log \gamma$ , the percentage of AN power for all these four schemes increases, which means more AN power is required to impair Eves when the transmit power is large. We also find that for the Random-IRS scheme and proposed algorithm, the percentage of AN power with the full CSI errors is larger than that with the partial CSI errors, and the gap grows with  $\log \gamma$ . When  $\log \gamma$  is small, the AN percentage with both the full and partial CSI errors is low, which means that the CSI errors can impair the Eves effectively.

#### E. Transmit Power Versus the Maximum Tolerable Channel Capacity of the Eavesdroppers

Fig. 6 depicts the transmit power versus the maximum tolerable channel capacity  $\log \beta$  of the Eves by assuming that the minimum channel capacity of the legitimate user is  $\log \gamma = 4$  bit/s/Hz. It is observed that the transmit power monotonically decreases with  $\log \beta$ , and the decreasing speed

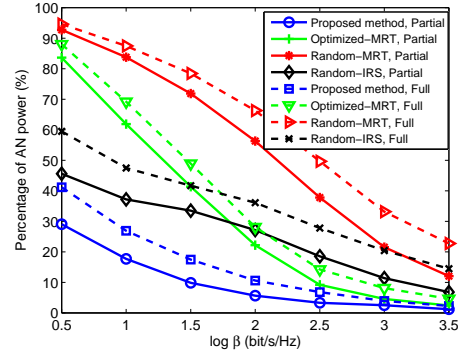
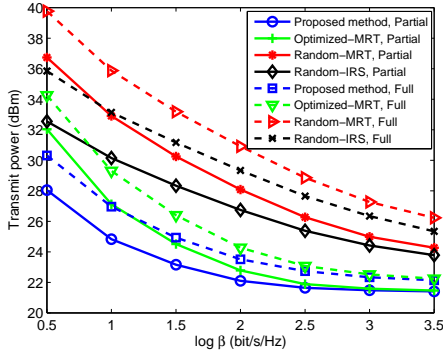


Fig. 6. Transmit power versus the maximum tolerable channel capacity  $\log \beta$  of the eavesdropper with  $N_t = 2$ ,  $M = 15$ , capacity  $\log \beta$  of the eavesdropper with  $N_t = 2$ ,  $M = 15$ ,  $K = 2$  and  $\log \gamma = 4$  bit/s/Hz. For partial Eves' CSI error, the normalized CSI error is  $\delta_{g,k} = 0.01$ ,  $\forall k$ , and for full Eves' CSI error, the normalized CSI error is  $\delta_{g,k} = \delta_{h,k} = 0.01$ ,  $\forall k$ .

slows down with increased  $\log \gamma$ . Increasing  $\log \beta$  means that the limitation on the information leakage for Eves is relaxed, thus less AN power and transmit power are required. The transmit power of the proposed algorithm is still the lowest compared with other schemes. However, when  $\log \beta$  is large enough, the transmit power of the Optimized-MRT scheme approaches that of the proposed algorithm. This means that it is not necessary to steer the AN towards Eves' direction by the proposed algorithm, but is enough to transmit almost isotropically distributed spatial noise by MRT strategy to interfere Eves when the data rate requirement for Eves is loose. Similarly, the Random-MRT scheme approaches that of the Random-IRS scheme when  $\log \beta$  is large. However, the transmit power of the Optimized-MRT scheme and the proposed algorithm is much lower than that of the Random-MRT scheme and Random-IRS scheme, which demonstrates the necessity of optimizing the phase shifts of the IRS. It is also found that the transmit power with full CSI errors is higher than that with partial CSI errors, and the gap is narrowed gradually with  $\log \beta$ .

The percentage of AN power in the total transmit power versus the maximum tolerable channel capacity  $\log \beta$  of the Eves is depicted in Fig. 7. It is shown that the required AN power decreases with  $\log \beta$ . The tighter the information leakage limitation for Eves is, the more AN power is required. The AN power of the proposed algorithm and Random-IRS scheme is less than that of the Optimized-MRT and Random-MRT, which means that the idea of making AN spatially focused is beneficial for reducing the transmit power. When  $\log \beta$  is large enough (e.g., 3.5 bit/s/Hz), the required AN power of the Optimized-MRT scheme approaches that of the proposed algorithm since the data rate requirement for Eves is greatly relaxed. In addition, the AN power required

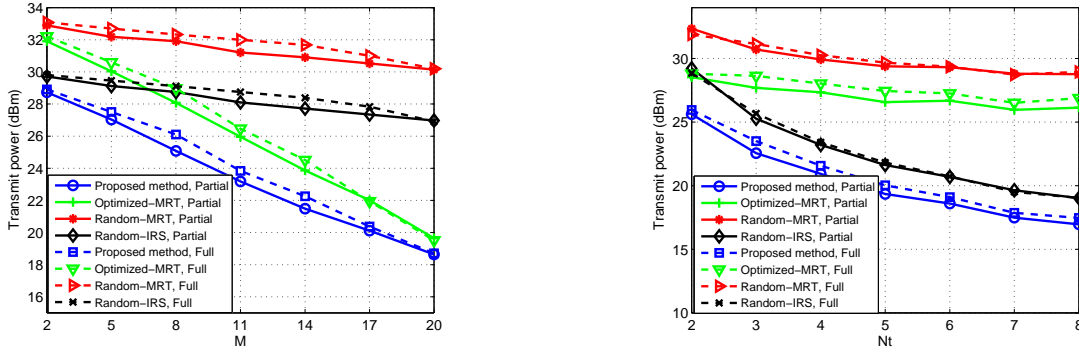


Fig. 8. Transmit power versus the IRS element number  $M$  with Fig. 9. Transmit power versus transmit antenna number  $N_t$  with  $N_t = 2$ ,  $K = 2$ ,  $\log \beta = 1$  bit/s/Hz and  $\log \gamma = 3$  bit/s/Hz. For  $M = 8$ ,  $K = 2$ ,  $\log \beta = 1$  bit/s/Hz and  $\log \gamma = 3$  bit/s/Hz. For partial Eves' CSI error, the normalized CSI error is  $\delta_{g,k} = 0.01$ , partial Eves' CSI error, the normalized CSI error is  $\delta_{g,k} = 0.01$ ,  $\forall k$ , and for full Eves' CSI error, the normalized CSI error is  $\forall k$ , and for full Eves' CSI error, the normalized CSI error is  $\delta_{g,k} = \delta_{h,k} = 0.01$ ,  $\forall k$ .

with the full CSI errors is higher than that with the partial CSI errors.

#### F. Transmit Power Versus the Number of IRS Elements

The minimum transmit power consumption versus different numbers of IRS elements is investigated in Fig. 8. It is observed that the transmit power is reduced with more IRS elements for all these schemes. The robust transmission design of the proposed algorithm outperforms the other schemes in terms of the lowest transmit power budget. The transmit power consumption of the proposed algorithm and the Optimized-MRT scheme drops much faster than that of the Random-IRS scheme and Random-MRT scheme, which demonstrate the effectiveness of optimizing the phase shifts of the IRS. When  $M$  is large, the transmit power of the Optimized-MRT tends to approach the transmit power of the proposed algorithm. This is because larger  $M$  brings more cascaded CSI errors, which enhance the capability of impairing Eves by the MRT strategy. The transmit power with the full CSI errors is slightly larger than that with the partial CSI errors.

#### G. Transmit Power Versus the Number of Transmit Antennas

The transmit power consumption versus different number of transmit antennas  $N_t$  is shown in Fig. 9. It is shown that the transmit power budget decreases with  $N_t$  for all these schemes. This is because more transmit antennas can reduce the transmit power budget even in the robust design problem. It is also observed that the proposed algorithm and the Random-IRS scheme are much more sensitive to  $N_t$  than the Optimized-MRT scheme and Random-MRT scheme. This is because

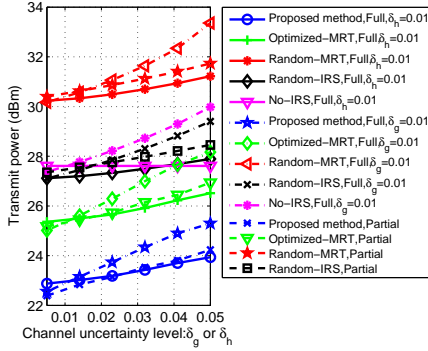


Fig. 10. Transmit power versus normalized CSI error variance  $\delta^2$  with  $N_t = 2$ ,  $M = 12$ ,  $K = 3$ ,  $\log \beta = 1$  bit/s/Hz and variance  $\delta^2$  with  $N_t = 2$ ,  $M = 12$ ,  $K = 2$ ,  $\log \beta = 1$  bit/s/Hz and  $\log \gamma = 3$  bit/s/Hz.

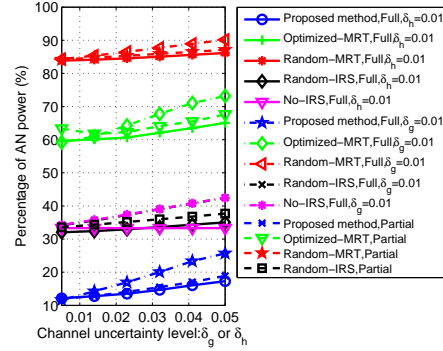


Fig. 11. Percentage of AN power versus normalized CSI error variance  $\delta^2$  with  $N_t = 2$ ,  $M = 12$ ,  $K = 2$ ,  $\log \beta = 1$  bit/s/Hz and  $\log \gamma = 3$  bit/s/Hz.

a larger  $N_t$  is helpful for increasing the Bob's data rate, but is not conducive to decrease the Eves' data rate. For the MRT strategy, the AN power is almost isotropically distributed, which is less effective to reduce the transmit power consumption when  $N_t$  is large. Thus, the transmit power of the Optimized-MRT scheme and Random-MRT scheme reduces very slowly. The transmit power with the full CSI errors is slightly higher than that with the partial CSI errors.

#### H. Transmit Power Versus CSI Uncertainty

Fig. 10 shows the transmit power versus the normalized CSI error  $\delta$ , where the normalized CSI errors of different eavesdroppers are assumed to be identical, i.e.,  $\delta_{g,k} = \delta, \forall k$ . As observed in Fig. 10, the transmit power consumption increases with the normalized CSI errors  $\delta$ , which means more transmit power is required when the channel quality degrades. When the normalized CSI error is relatively small, the transmit power with full CSI errors is slightly higher than that with partial CSI errors. When the normalized CSI error is relatively large, the transmit power with full CSI errors is slightly lower than that with full CSI errors. This means that when the CSI error is large, the full CSI errors are preferred to impair the Eves. When full CSI errors exist for Eves, the transmit power changing with the CSI error on the direct link is higher than that changing with the CSI error on the reflecting link. This means that the transmit power is more sensitive to the CSI error on the direct link. The power budget of the proposed algorithm is much lower than that of the other three schemes. By comparing with the No-IRS scheme, it shows that the security performance of the IRS-aided communication system is much better than the no-IRS system even with CSI errors in both the direct link and IRS link.

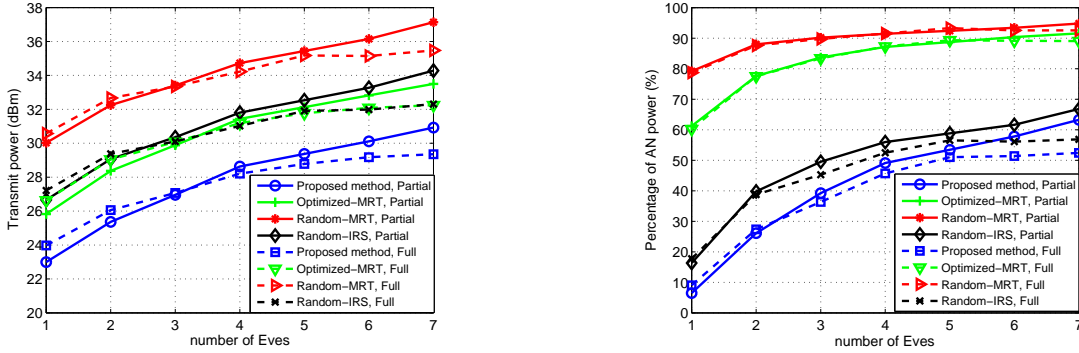


Fig. 12. Transmit power versus the number of Eves  $K$  with Fig. 13. Percentage of AN power versus the number of Eves  $K$   $N_t = 2$ ,  $M = 8$ , and  $\log \beta = 1$  bit/s/Hz and  $\log \gamma = 3$  bit/s/Hz. For partial Eves' CSI error, the normalized CSI error is  $\delta_{g,k} = 0.01$ ,  $\forall k$ , and for full Eves' CSI error, the normalized CSI error is  $\delta_{g,k} = \delta_{h,k} = 0.01$ ,  $\forall k$ .

Fig. 11 gives the percentage of AN power in the total transmit power versus the normalized CSI error  $\delta$ . It is shown that more AN power is required for larger CSI errors. When the CSI errors exist, the AN power required by the proposed algorithm is much lower than that without IRS, which demonstrates the benefits of exploiting the IRS. Moreover, the AN power required by the CSI error on the direct link is higher than that required by the CSI error on the IRS link.

### I. Transmit Power Versus the Number of Eves

The transmit power versus the number of Eves is shown in Fig. 12. It is observed that the transmit power consumption increases with the number of Eves for all these schemes. When the number of Eves is relatively small, the transmit power with partial CSI errors is slightly lower than that with full CSI errors, which means that the partial CSI error is enough to impair the Eves. When the number of Eves is relatively large, the transmit power with partial CSI errors is slightly higher than that with full CSI errors, which means the full CSI error is preferred to further interfere more Eves.

The percentage of AN power in the total transmit power versus the number of Eves  $K$  is given in Fig. 13. As observed from Fig. 13, the AN power increases with the number of Eves for all these schemes. When the number of Eves increases, the transmit antenna does not have enough degrees of freedom (DOF) to interfere the Eves, thus the AN power has to be increased. When  $K$  is relatively large, the AN power with the full CSI errors is slightly lower than that with the partial CSI errors. This means that when there are more Eves, the full CSI errors are preferred to

further interfere the Eves. Compared with other schemes, the AN power required by the proposed algorithm is the lowest, which confirms the superiority of the proposed algorithm.

## V. CONCLUSION

In this paper, we designed the outage constrained robust transmission in the secure IRS-aided wireless communications by considering the statistical CSI errors on both direct links and IRS reflecting links to Eves. An OC-PM problem was formulated to minimize the transmit power by jointly optimizing the transmit beamforming vector, AN covariance, and IRS phase shifts. To solve it, the BTI and AO methods were utilized. Some mathematical manipulations were proposed to transform the optimization problem for IRS phase shifts to be convex. Then the SDR and CCP algorithms were exploited. Simulations verified the superiority of the proposed algorithm over the benchmark schemes.

### APPENDIX A

#### PROOF OF (34d)

By utilizing the rank properties  $\text{rank}\{\mathbf{AB}\} \leq \min\{\text{rank}(\mathbf{A}), \text{rank}(\mathbf{B})\}$  and  $\text{rank}(\mathbf{A} \otimes \mathbf{B}) = \text{rank}(\mathbf{A}) \cdot \text{rank}(\mathbf{B})$ , we can prove  $\lambda_{\min}\{\Sigma_{e,k}^{1/2}((c_g \mathbf{I}_{N_t})^T \otimes \mathbf{E})\Sigma_{e,k}^{1/2}\} = 0$  as follows.

We have the inequality of  $\text{rank}\{\Sigma_{ge,k}^{1/2}((c_g \mathbf{I}_{N_t})^T \otimes \mathbf{E})\Sigma_{ge,k}^{1/2}\} \leq \min\{\text{rank}(\Sigma_{ge,k}^{1/2}), \text{rank}((c_g \mathbf{I}_{N_t})^T \otimes \mathbf{E})\}$ . Since  $\text{rank}((c_g \mathbf{I}_{N_t})^T \otimes \mathbf{E}) = \text{rank}(c_g \mathbf{I}_{N_t}) \cdot \text{rank}(\mathbf{E}) = N_t$ , we have  $\text{rank}\{\Sigma_{ge,k}^{1/2}((c_g \mathbf{I}_{N_t})^T \otimes \mathbf{E})\Sigma_{ge,k}^{1/2}\} \leq N_t$ . Since the matrix  $\Sigma_{ge,k}^{1/2}((c_g \mathbf{I})^T \otimes \mathbf{E})\Sigma_{ge,k}^{1/2}$  is an  $MN_t \times MN_t$  dimensional semidefinite matrix, its minimum eigenvalue is zero as

$$\lambda_{\min}\{\Sigma_{ge,k}^{1/2}((c_g \mathbf{I})^T \otimes \mathbf{E})\Sigma_{ge,k}^{1/2}\} = 0. \quad (66)$$

### APPENDIX B

#### PROOF OF (55)

The derivations in the step of  $(m)$  are given as follows:

$$\begin{aligned} & \left\| \Sigma_{ge,k}^{1/2T} (\Xi_e \otimes \phi) \Sigma_{he,k}^{1/2} \right\|^2 \stackrel{(m_1)}{=} \text{Tr}[\Sigma_{ge,k}^{1/2T} (\Xi_e \otimes \phi) \Sigma_{he,k}^{1/2} \Sigma_{he,k}^{1/2} (\Xi_e \otimes \phi)^H \Sigma_{ge,k}^{1/2*}] \\ & = \text{Tr}[(\Xi_e \otimes \phi)^H \Sigma_{ge,k}^* (\Xi_e \otimes \phi) \Sigma_{he,k}] \\ & \stackrel{(m_2)}{=} \text{vec}^H(\Xi_e \otimes \phi) (\Sigma_{he,k}^T \otimes \Sigma_{ge,k}^*) \text{vec}(\Xi_e \otimes \phi) \\ & = \text{vec}^H(\Xi_e \otimes \phi) [(\Sigma_{he,k}^{1/2T} \Sigma_{he,k}^{1/2T}) \otimes (\Sigma_{ge,k}^{1/2*} \Sigma_{ge,k}^{1/2*})] \text{vec}(\Xi_e \otimes \phi) \\ & = \text{vec}^H(\Xi_e \otimes \phi) [(\Sigma_{he,k}^{1/2T} \otimes \Sigma_{ge,k}^{1/2*})^H (\Sigma_{he,k}^{1/2T} \otimes \Sigma_{ge,k}^{1/2*})] \text{vec}(\Xi_e \otimes \phi) \\ & = \left\| (\Sigma_{he,k}^{1/2T} \otimes \Sigma_{ge,k}^{1/2*}) \text{vec}(\Xi_e \otimes \phi) \right\|^2. \end{aligned} \quad (67)$$

$$\begin{aligned}
& \left\| \Sigma_{ge,k}^{1/2T} (\Xi_e \otimes \mathbf{E}^T) \Sigma_{ge,k}^{1/2*} \right\|^2 \stackrel{(m_1)}{=} \text{Tr}[\Sigma_{ge,k}^{1/2T} (\Xi_e \otimes \mathbf{E}^T) \Sigma_{ge,k}^{1/2*} \Sigma_{ge,k}^{1/2T} (\Xi_e \otimes \mathbf{E}^*) \Sigma_{ge,k}^{1/2*}] \\
& = \text{Tr}[(\Xi_e \otimes \mathbf{E}^T)^H \Sigma_{ge,k}^* (\Xi_e \otimes \mathbf{E}^T) \Sigma_{ge,k}^*] \\
& \stackrel{(m_2)}{=} \text{vec}^H(\Xi_e \otimes \mathbf{E}^T) (\Sigma_{ge,k} \otimes \Sigma_{ge,k}^*) \text{vec}(\Xi_e \otimes \mathbf{E}^T) \\
& = \text{vec}^H(\Xi_e \otimes \mathbf{E}^T) [(\Sigma_{ge,k}^{1/2} \Sigma_{ge,k}^{1/2}) \otimes (\Sigma_{ge,k}^{1/2*} \Sigma_{ge,k}^{1/2*})] \text{vec}(\Xi_e \otimes \mathbf{E}^T) \\
& = \text{vec}^H(\Xi_e \otimes \mathbf{E}^T) [(\Sigma_{ge,k}^{1/2} \otimes \Sigma_{ge,k}^{1/2*})^H (\Sigma_{ge,k}^{1/2} \otimes \Sigma_{ge,k}^{1/2*})] \text{vec}(\Xi_e \otimes \mathbf{E}^T) \\
& = \left\| (\Sigma_{ge,k}^{1/2} \otimes \Sigma_{ge,k}^{1/2*}) \text{vec}(\Xi_e \otimes \mathbf{E}^T) \right\|^2. \tag{68}
\end{aligned}$$

$$\begin{aligned}
& \left\| \Sigma_{he,k}^{1/2} \Xi_e \Sigma_{he,k}^{1/2} \right\|^2 \stackrel{(m_1)}{=} \text{Tr}[\Sigma_{he,k}^{1/2} \Xi_e \Sigma_{he,k}^{1/2} \Sigma_{he,k}^{1/2} \Xi_e \Sigma_{he,k}^{1/2}] \\
& = \text{Tr}[\Xi_e \Sigma_{he,k} \Xi_e \Sigma_{he,k}] \\
& \stackrel{(m_2)}{=} \text{vec}^H(\Xi_e) (\Sigma_{he,k}^T \otimes \Sigma_{he,k}) \text{vec}(\Xi_e) \\
& = \text{vec}^H(\Xi_e) [(\Sigma_{he,k}^{1/2T} \Sigma_{he,k}^{1/2T}) \otimes (\Sigma_{he,k}^{1/2} \Sigma_{he,k}^{1/2})] \text{vec}(\Xi_e) \\
& = \text{vec}^H(\Xi_e) [(\Sigma_{he,k}^{1/2T} \otimes \Sigma_{he,k}^{1/2})^H (\Sigma_{he,k}^{1/2T} \otimes \Sigma_{he,k}^{1/2})] \text{vec}(\Xi_e) \\
& = \left\| (\Sigma_{he,k}^{1/2T} \otimes \Sigma_{he,k}^{1/2}) \text{vec}(\Xi_e) \right\|^2. \tag{69}
\end{aligned}$$

where  $(m_1)$  is due to  $\|\mathbf{A}\|_F^2 = \text{Tr}[\mathbf{A}\mathbf{A}^H]$ , and  $(m_2)$  is obtained by invoking the identity  $\text{Tr}(\mathbf{A}^H \mathbf{B} \mathbf{C} \mathbf{D}) = \text{vec}^H(\mathbf{A})(\mathbf{D}^T \otimes \mathbf{B}) \text{vec}(\mathbf{C})$ .

## APPENDIX C

### PROOF OF LEMMA 2

We define a matrix  $\mathbf{C} = \mathbf{a}\mathbf{b}^T$ , where  $\mathbf{a}$  and  $\mathbf{b}$  are vectors. Since we have  $\text{vec}(\mathbf{C}) = \mathbf{b} \otimes \mathbf{a}$ , then we have

$$\begin{aligned}
\|\mathbf{C}\|_F &= \|\mathbf{b} \otimes \mathbf{a}\|_2 = \sqrt{\text{Tr}(\mathbf{C}\mathbf{C}^H)} = \sqrt{\text{Tr}(\mathbf{a}\mathbf{b}^T \mathbf{b}^* \mathbf{a}^H)} \\
&= \sqrt{\mathbf{b}^T \mathbf{b}^* \mathbf{a}^H \mathbf{a}} = \|\mathbf{b}\|_2 \|\mathbf{a}\|_2. \tag{70}
\end{aligned}$$

## APPENDIX D

### PROOF OF THAT $\mathbf{B}_{e,k}$ IS RANK DEFICIENT

We can prove  $\lambda_{\min}\{\mathbf{B}_{e,k}\} = 0$  as follows:

We have

$$\lambda_{\min}\{\mathbf{B}_{e,k}\} = \lambda_{\min} \left\{ \begin{bmatrix} \Sigma_{he,k}^{1/2} c_g^{1/2} \mathbf{I}_{N_t} \\ \Sigma_{ge,k}^{1/2T} (c_g^{1/2} \mathbf{I}_{N_t} \otimes \phi) \end{bmatrix} \begin{bmatrix} c_g^{1/2} \mathbf{I}_{N_t} \Sigma_{he,k}^{1/2} & (c_g^{1/2} \mathbf{I}_{N_t} \otimes \phi^H) \Sigma_{ge,k}^{1/2*} \end{bmatrix} \right\}. \tag{71}$$

We find

$$\begin{aligned}
\text{rank}\{\mathbf{B}_{e,k}\} &\leq \text{rank}\left\{\left[\begin{array}{cc} c_g^{1/2}\mathbf{I}_{N_t}\Sigma_{he,k}^{1/2} & (c_g^{1/2}\mathbf{I}_{N_t}\otimes\phi^H)\Sigma_{ce,k}^{1/2*} \end{array}\right]\right\} \\
&\leq \text{rank}\{c_g^{1/2}\mathbf{I}_{N_t}\Sigma_{he,k}^{1/2}\} + \text{rank}\{(c_g^{1/2}\mathbf{I}_{N_t}\otimes\phi^H)\Sigma_{ce,k}^{1/2*}\} \\
&\leq 2N_t,
\end{aligned} \tag{72}$$

where the rank properties  $\text{rank}(\mathbf{AB}) \leq \min\{\text{rank}(\mathbf{A}), \text{rank}(\mathbf{B})\}$  and  $\text{rank}([\mathbf{A}, \mathbf{B}]) \leq \text{rank}(\mathbf{A}) + \text{rank}(\mathbf{B})$  are utilized. Since the matrix  $\mathbf{B}_{e,k}$  is a  $(MN_t + N_t) \times (MN_t + N_t)$  dimensional semidefinite matrix, its minimum eigenvalue is zero as  $\lambda_{\min}\{\mathbf{B}_{e,k}\} = 0$ .

### REFERENCES

- [1] Q. Wu and R. Zhang, "Towards smart and reconfigurable environment: Intelligent reflecting surface aided wireless network," *IEEE Communications Magazine*, vol. 58, no. 1, pp. 106–112, 2019.
- [2] C. Pan, H. Ren, K. Wang, M. ElKashlan, M. Chen, D. Renzo, Y. Hao, J. Wang, A. Swindlehurst, X. You, and H. Lajos, "Reconfigurable intelligent surface for 6G and beyond: Motivations, principles, applications, and research directions." [Online]. Available: <https://arxiv.org/abs/2011.04300>
- [3] T. J. Cui, M. Q. Qi, X. Wan, J. Zhao, and Q. Cheng, "Coding metamaterials, digital metamaterials and programmable metamaterials," *Light: Science & Applications*, vol. 3, no. 10, pp. 218–218, 2014.
- [4] M. Di Renzo, K. Ntontin, J. Song, F. H. Danufane, X. Qian, F. Lazarakis, J. De Rosny, D.-T. Phan-Huy, O. Simeone, R. Zhang *et al.*, "Reconfigurable intelligent surfaces vs. relaying: Differences, similarities, and performance comparison," *IEEE Open Journal of the Communications Society*, vol. 1, pp. 798–807, 2020.
- [5] C. Pan, H. Ren, K. Wang, W. Xu, M. ElKashlan, A. Nallanathan, and L. Hanzo, "Multicell MIMO communications relying on intelligent reflecting surfaces," *IEEE Transactions on Wireless Communications*, vol. 19, no. 8, pp. 5218–5233, 2020.
- [6] C. Pan, H. Ren, K. Wang, M. ElKashlan, A. Nallanathan, J. Wang, and L. Hanzo, "Intelligent reflecting surface aided MIMO broadcasting for simultaneous wireless information and power transfer," *IEEE Journal on Selected Areas in Communications*, vol. 38, no. 8, pp. 1719–1734, 2020.
- [7] T. Bai, C. Pan, Y. Deng, M. ElKashlan, A. Nallanathan, and L. Hanzo, "Latency minimization for intelligent reflecting surface aided mobile edge computing," *IEEE Journal on Selected Areas in Communications*, vol. 38, no. 11, pp. 2666–2682, 2020.
- [8] G. Zhou, C. Pan, H. Ren, K. Wang, and A. Nallanathan, "Intelligent reflecting surface aided multigroup multicast MISO communication systems," *IEEE Transactions on Signal Processing*, vol. 68, pp. 3236–3251, 2020.
- [9] L. Zhang, Y. Wang, W. Tao, Z. Jia, T. Song, and C. Pan, "Intelligent reflecting surface aided MIMO cognitive radio systems," *IEEE Transactions on Vehicular Technology*, vol. 69, no. 10, pp. 11 445–11 457, 2020.
- [10] X. Yu, D. Xu, and R. Schober, "Enabling secure wireless communications via intelligent reflecting surfaces," in *2019 IEEE Global Communications Conference (GLOBECOM)*, 2019, pp. 1–6.
- [11] J. Chen, Y.-C. Liang, Y. Pei, and H. Guo, "Intelligent reflecting surface: A programmable wireless environment for physical layer security," *IEEE Access*, vol. 7, pp. 82 599–82 612, 2019.
- [12] L. Dong and H. Wang, "Secure MIMO transmission via intelligent reflecting surface," *IEEE Wireless Communications Letters*, vol. 9, no. 6, pp. 787–790, 2020.
- [13] M. Cui, G. Zhang, and R. Zhang, "Secure wireless communication via intelligent reflecting surface," *IEEE Wireless Communications Letters*, vol. 8, no. 5, pp. 1410–1414, 2019.

- [14] X. Guan, Q. Wu, and R. Zhang, "Intelligent reflecting surface assisted secrecy communication: Is artificial noise helpful or not?" *IEEE Wireless Communications Letters*, vol. 9, no. 6, pp. 778–782, 2020.
- [15] S. Hong, C. Pan, H. Ren, K. Wang, and A. Nallanathan, "Artificial-noise-aided secure MIMO wireless communications via intelligent reflecting surface," *IEEE Transactions on Communications*, vol. early access, pp. 1–17, 2020.
- [16] Z. Chu, W. Hao, P. Xiao, and J. Shi, "Intelligent reflecting surface aided multi-antenna secure transmission," *IEEE Wireless Communications Letters*, vol. 9, no. 1, pp. 108–112, 2019.
- [17] D. Xu, X. Yu, Y. Sun, D. W. K. Ng, and R. Schober, "Resource allocation for secure IRS-assisted multiuser MISO systems," in *2019 IEEE Globecom Workshops (GC Wkshps)*. IEEE, 2019, pp. 1–6.
- [18] A. Taha, M. Alrabeiah, and A. Alkhateeb, "Enabling large intelligent surfaces with compressive sensing and deep learning." [Online]. Available: <https://arxiv.org/abs/1904.10136>
- [19] Z. Zhou, N. Ge, Z. Wang, and L. Hanzo, "Joint transmit precoding and reconfigurable intelligent surface phase adjustment: A decomposition-aided channel estimation approach," *IEEE Transactions on Communications*, vol. early access, pp. 1–15, 2020.
- [20] Z. Wang, L. Liu, and S. Cui, "Channel estimation for intelligent reflecting surface assisted multiuser communications: Framework, algorithms, and analysis," *IEEE Transactions on Wireless Communications*, vol. 19, no. 10, pp. 6607–6620, 2020.
- [21] P. Wang, J. Fang, H. Duan, and H. Li, "Compressed channel estimation for intelligent reflecting surface-assisted millimeter wave systems," *IEEE Signal Processing Letters*, vol. 27, pp. 905–909, 2020.
- [22] J. Chen, Y.-C. Liang, H. V. Cheng, and W. Yu, "Channel estimation for reconfigurable intelligent surface aided multi-user MIMO systems." [Online]. Available: <https://arxiv.org/abs/1912.03619>
- [23] S. Zhang and R. Zhang, "Capacity characterization for intelligent reflecting surface aided MIMO communication," *IEEE Journal on Selected Areas in Communications*, vol. 38, no. 8, pp. 1823–1838, 2020.
- [24] G. Zhou, C. Pan, H. Ren, K. Wang, M. D. Renzo, and A. Nallanathan, "Robust beamforming design for intelligent reflecting surface aided MISO communication systems," *IEEE Wireless Communications Letters*, vol. 9, no. 10, pp. 1658–1662, 2020.
- [25] X. Yu, D. Xu, Y. Sun, D. W. K. Ng, and R. Schober, "Robust and secure wireless communications via intelligent reflecting surfaces," *IEEE Journal on Selected Areas in Communications*, vol. 38, no. 11, pp. 2637–2652, 2020.
- [26] G. Zhou, C. Pan, H. Ren, K. Wang, and A. Nallanathan, "A framework of robust transmission design for IRS-aided MISO communications with imperfect cascaded channels," *IEEE Transactions on Signal Processing*, vol. 68, pp. 5092–5106, 2020.
- [27] X. Yu, D. Xu, D. W. K. Ng, and R. Schober, "IRS-assisted green communication systems: Provable convergence and robust optimization," 2020. [Online]. Available: <https://arxiv.org/abs/2011.06484>
- [28] T. A. Le, T. Van Chien, and M. Di Renzo, "Robust probabilistic-constrained optimization for IRS-aided MISO communication systems," *IEEE Wireless Communications Letters*, vol. early access, pp. 1–5, 2020.
- [29] L. Zhang, C. Pan, Y. Wang, H. Ren, K. Wang, and A. Nallanathan, "Robust beamforming design for intelligent reflecting surface aided cognitive radio systems with imperfect cascaded CSI," 2020. [Online]. Available: <https://arxiv.org/abs/2004.04595>
- [30] S. Hong, C. Pan, H. Ren, K. Wang, K. K. Chai, and A. Nallanathan, "Robust transmission design for intelligent reflecting surface aided secure communication systems with imperfect cascaded CSI," 2020. [Online]. Available: <https://arxiv.org/abs/2004.11580>
- [31] K.-Y. Wang, A. M.-C. So, T.-H. Chang, W.-K. Ma, and C.-Y. Chi, "Outage constrained robust transmit optimization for multiuser MISO downlinks: Tractable approximations by conic optimization," *IEEE Transactions on Signal Processing*, vol. 62, no. 21, pp. 5690–5705, 2014.

- [32] 3GPP, “Technical specification group radio access network; study on 3D channel model for LTE (release 12),” TR 36.873 V12.7.0, Tech. Rep., Dec. 2017.
- [33] W.-C. Liao, T.-H. Chang, W.-K. Ma, and C.-Y. Chi, “QoS-based transmit beamforming in the presence of eavesdroppers: An optimized artificial-noise-aided approach,” *IEEE Transactions on Signal Processing*, vol. 59, no. 3, pp. 1202–1216, 2010.